Prepared for:

WL | Delft Hydraulics

Analysis field measurements Paulina Polder:

Looking for sediment-fluid interaction

G.J. de Boer and J.C. Winterwerp

Research Report

December 2003

WL | delft hydraulics

CLIENT: WL | Delft Hydraulics

TITLE: Analysis field measurements Paulina Polder: Looking for sediment-fluid interaction

ABSTRACT:

The area of intertidal areas in the Netherlands has tremendously decreased over the last decades. For management of the remaining area of inter tidal areas, knowledge of how these basins catch sediment is indispensable. One of the processes which is expected to be responsible for catching fine sediment on intertidal areas is part of this study: the interaction between turbulence and sediment induced buoyancy effects, which might lead to sediment-induced density currents and the possible collapse of the turbulence field and concentration profile when the saturation concentration is exceeded.

In this project this feed-back mechanism is investigated by means of a data analysis. The data analysis concerned velocity, turbidity and water level measurements at the Paulina intertidal area in the WesterScheldt. The velocity and turbidity data were collected at two levels. This allows one to gain information on vertical gradients. The generation of density currents was expected to be visible in the vertical concentration gradients. Unfortunately, due to an inadequate calibration of the turbidity sensors, the concentration values near the bed are larger than the ones higher in the water column. This makes it impossible to say anything about vertical gradients in concentration the profile from the data. The conclusions from the data analysis are:

1) The supposed collapse of the entire concentration profile and of the turbulent fluctuations did not occur in the measurements. Possibly the concentrations were too low for this effect to occur.
2) Another phenomenon may indicate the presence of sediment-induced effects: many velocities recordings show a 10 to 30 degree veering with height, possibly indicating the presence of a density current. The hypothesis is that a bottom density current is formed by the interaction between turbulence and sediment concentration. This under-current is then directed by local topography, while the higher layer is governed by larger scale hydrodynamic features. However, the veering may also be the result of wind and/or Coriolis effects. It is recommended to focus further research on this observation.
3) Maximum sediment fluxes on the tidal flats seem to occur in the shallows (< 0.5 deep, at the beginning and end of immersion), when concentrations, velocities and turbulence are largest. Any residual sediment transport is therefore determined as the difference between the large values of the ebb and flood fluxes. This is in accordance with Christie et al. (1999)

A strategy for further research is to start with sensitivity research with numerical models to find the actual cause for the veering of the velocity with height. After this it is recommend to start a new field measurement campaign.

REFERENCES: Doelsubsidie V&W / OC&W.

VER.	ORIGINATOR		DATE	REMARKS	REVIEW		APPROVED BY	
1.0	G.J. de Boer		23 December 2002		C. Kuijper		T. Schilperoort	
	J.C. Winterwerp							

PROJECT IDENTIFICATION:	Z3506
KEYWORDS:	Paulina Polder, WesternScheldt, sediment-fluid interaction, turbulence, density current, tidal flat, tidal marsh
NUMBER OF PAGES	26 with 2 appendices of in total 17 pages.
CONFIDENTIAL:	☐ YES, until (date) ☒ NO
STATUS:	☐ PRELIMINARY ☐ DRAFT ☒ FINAL

Contents

1 Introduction

Over the last century, the coverage of intertidal areas in the Netherlands has shown a dramatic decline. The Wadden Sea, the Westerscheldt, a reduced Easternscheldt and the Nieuwe Maas have remained, but a large amount of intertidal areas has been lost: Veerse Gat, Brielse Gat, Markiezaat, Eendracht, Grevelingen, Biesbosch, Hollandsch Diep, Lauwerszee en Zuiderzee (Lake IJssel). Prof. dr. Saeijs once calculated the intertidal area coverage to be 866.000 hectare around 1900. Less than 50 % of these areas have remained up to present: 393.000 hectares. Still now, annually 50 out of 12.000 hectares dissappear in the Eastern Scheldt. Without countermeasures, after two centuries there will be no intertidal area left in the Eastern Scheldt at this pace. [NRC Handelsblad, 11,12 nov 2003]. Knowledge of the behaviour of sediments in coastal seas and estuaries, ranging from sand to silt and clays, is of paramount importance for the management of these valuable, disappearing areas. Modelling the behaviour of fines in these tidal basins requires knowledge of (i) the sediment fluxes into these basins, (ii) the net accumulation within these basins (huge fluxes can still give a zero accumulation) as well as (iii) the distribution of sediment over these basins (in the channels or rather on the tidal flats).

Given the importance of modelling fine sediment fluxes in tidal basins, the following question rises: are we able to model fine sediment fluxes properly at present? At present the answer to this question is no. For instance, the transport of fine cohesive sediment towards the Wadden Sea, the exchange of fine sediment between North Sea and Wadden Sea and the sediment processes within the Wadden Sea were not modelled properly in Phase 1 of the FLYLAND/ONL study. This was evident from the computed sediment fluxes through the Marsdiep and the computed SPM-concentrations within the Wadden Sea. From a preliminary analysis of the modelling approach and model results, it was concluded that a proper modelling of the North Sea – Wadden Sea sediment exchange requires a proper modelling of the sediment processes within the Wadden Sea in general, and of the water-bed exchange processes in particular.

At present some new developments in the field of cohesive sediments engineering and science are starting to accelerate. These topics may very well form the solution to the inability to model fine sediment fluxes properly. These topics are, among others, the research on and modelling of influence of biological activity on erosion and deposition behaviour, the modelling of fluid mud layers for calculating the trapping efficiency of harbours, the conceptual improvement and pilot implementation of water bed models dealing with the influence of consolidation on erosion. This R&D project deals with yet another new item in this list: the interaction between sediment and flow (turbulence), supposed to be a large catching mechanism for sediment in shallow waters. Generally mud flats look extra-ordinarily smooth, as if fluid mud has been poured over the flats. The interaction between sediment and flow may in some cases lead to a collapse of the sediment profile, which generates a density current. This density current is supposed to be responsible for the smooth surface of intertidal areas.

1.1 R&D framework

This research project is part of the Delft Hydraulics R&D integration project *Effect Chain Wadden Sea*. In this overall project several other research projects are executed:

- Morphological model Westerschelde
- DELOS (effect of vegetation on hydrodynamics)
- Biogeomorphology Westerschelde
- Behaviour of sand-mud mixtures
- Sensitivity analysis Wadden Sea
- Ecology of higher trophic levels
- Sediment Water Interaction (a.o. development generic water bed model Delwaq-g)

Together, these projects cover the three main areas of application of cohesive sediment research: water quality, ecology and morphology. There are two main reasons for the project *Intertidal Areas* to participate in *Effect Chain Wadden Sea*:

- The turbulence collapse mechanism investigated in this R&D project may explain a part of the missing sediment in the overall balance of the Wadden Sea mentioned in the previous section. However, this is only part of the story. More mechanisms are needed to trace all the 'lost' sediment. Contributing to the project *Effect Chain Wadden Sea* adds to the understanding and quantifying/predicting of the overall sediment balance of the Wadden Sea.
- It is known that both physical and biological processes influence the local (i.e. small scale) sedimentation and erosion characteristics of cohesive sediments in the Wadden Sea. Currently nearly all models dealing with sedimentation and erosion processes from a biological point of view assume a constant influence of physical parameters. An example of this approach is the so called 'cosinus forcing' of sediment concentrations assumed in algae models in the North Sea. On the other hand nearly all models dealing with erosion and deposition from a physical point of view assume a constant level of biological activity at present. The interactions between biology and physics are not incorporated in any of these models yet. The present project adds to the local reference framework of *Effect Chain Wadden Sea* for evaluating the relative importance of physical to non-physical processes as well as their interactions.

1.2 Transport processes in shallow basins

Generally, the suspended sediment concentrations in shallow basins, such as the Wadden Sea and in parts of the WesterScheldt, and in particular further into the system, are much larger than in the surrounding North Sea. This is the result of two mechanisms:

- the net sediment transport is (often) landwards (flood dominated) bringing marine sediments into and/or keeping fluviatile sediments within the system, and
- (part of) the sediment is not deposited on the bed of the estuary or lagoon, but remains in suspension.

Many studies have been published in the literature to explain the observed high turbidity in shallow areas, e.g. Van Straaten and Kuenen (1957), Postma (1967), Groen (1967), Dronkers (1984), who treated the fine-sediment processes in the Dutch Wadden Sea, as well as a number of non-Dutch authors, amongst which Kennedy (1984) and Dyer (1997). The various mechanisms described by these authors are:

- Gravitational circulation

- Tidal asymmetry and lag effects
- Water level effects
- Wave effects

When explaining the net sediment import of the Wadden Sea and the high turbidity levels with these mechanisms, a paradox is encountered: waves are necessary to explain high turbidity levels in the tidal basins, but they counteract net sediment import. These ideas can be tested with a simple model of a tidal inlet or estuary. It is noted that the observations of a net landward transport and augmented turbidity levels cannot be explained by the existence of particle, c.q. floc size distributions. In particular, the mechanisms above do not explain accumulation of the finest, mainly organic fraction in the system, because the non-flocculated part of this sediment will hardly settle, as its settling velocity is very small. Recently new mechanism that affect the import and export of fine sediment from tidal basin, and that can solve this paradox, have been proposed:

- Physical and biological seasonal effects
- Horizontal circulations
- Flocculation characteristics
- The combination of Krone's sedimentation rate and Partheniades' erosion rate, which is widely used, is in fact not valid.
- Sediment-flow interaction. This is the topic of the present project and is discussed in more detail in the next section.

1.3 Sediment-flow interaction

In flows with a high concentration of sediments (sediment-fluid mixtures), the settling velocity of a single sediment particle is reduced by the presence of other particles. In order to account for this so-called hindered settling effect, the settling velocity in a fluid-sediment mixture is generally modelled as a decaying function of increasing sediment concentration. Hindered settling results in the formation of interfaces, known as lutoclines. Around these lutoclines large gradients in density are formed, which cause significant damping of vertical mixing. Sediment-flow interactions occur when this turbulence damping becomes so strong that significant gradients in the vertical concentration profile are generated. As a result, horizontal gradients in near-bed concentrations can become large, triggering sediment-induced density currents. These sediment-induced density currents already play a role at sediment concentrations as low as 100 mg/l (Winterwerp and Van Kessel, 2002).

If the vertical gradients in the concentration profile become too large, the flow becomes super-saturated, i.e. the transport capacity of the flow is exceeded, and a total collapse of the turbulence field and concentration profile, with subsequent formation of fluid mud layers is expected. A theoretical relation for the so-called saturation concentration as a function of the water depth and the shear velocity has been derived by Winterwerp [2001]. This concept is based on the following sequence of occurrences.

When the carrying capacity (saturation concentration) for cohesive sediment is exceeded, a fluid mud layer is formed upon the deposition of cohesive sediment flocs. Thus a two layer fluid system develops causing significant damping of the vertical mixing process: the turbulence generated in the (thin) bottom layer cannot penetrate any more through the lutocline separating the high concentrated bottom layer from the overlying water. The thickness of the bottom layer is irrelevant in this case, only the steepness of the vertical concentration gradient matters. Subsequently, the damping of the vertical mixing

process decreases the carrying capacity further. This positive feedback results in a catastrophic collapse of the turbulence field and the concentration profile.

This phenomenon makes the behaviour of fines completely different from that of coarser sediments. When the sand sediment concentration in the water increases, the turbulence in the water will be damped by the increased buoyancy effect of the sediment. This reduction of the turbulence leads to a decrease in the carrying capacity of the flow, being a function of the upward turbulent mixing of sediment versus the downward settling velocity. The amount of sediment exceeding the carrying capacity will deposit on the waterbed. If sand grains deposit, they form a new rigid (and hence rough) layer on the bed that is equally productive in the generation of turbulence as the original bed. This turbulence can easily mix into the water column in the absence of a lutocline. Therefore a new, but lower equilibrium transport is established. There is no catastrophic feedback.

The saturation concentration (for cohesive sediments) for stationary flow derived by Winterwerp [1999] is proportional to the ratio of u_*^3/h. If sediment-laden water enters an intertidal area, both the water depth and the velocity decrease. The saturation concentration will therefore decrease since the nominator decreases faster than the denominator. Accordingly, the above-mentioned collapse of turbulence might be an important mechanism responsible for the trapping of sediment in the intertidal zone. Establishing the occurrence of this process as well as the conditions under which it can and does occur are the first objectives of this project.

These buoyancy effects due to sediment-fluid interaction affect the deposition process as follows:

a. As a result of a positive feed-back between the sediment suspension and turbulence mixing, sediment-induced buoyancy effects result in a total collapse of the mixing capacity of the flow, hence rapid sedimentation and the formation of small-scale sediment-induced density currents.
b. Toorman (1999) proposes that the boundary conditions for flow and turbulence equations should be modified to account for buoyancy effects properly, as a result of which these effects may be even larger than estimated by Winterwerp (2001). This is to be elaborated.
c. The positive feed-back mentioned above also affects the impact of waves:
    - the wave-boundary layer is affected, decreasing the contribution of this layer to the overall mixing capacity of the flow,
    - the waves are damped in the viscous, high-concentrated near-bed sediment suspension (fluid mud layer), decreasing their effect, and
    - the sediment deposits are protected from wave-induced erosion by aforementioned near-bed suspension.

The first two mechanisms (a,b) of this list will be dealt with in this R&D project.

2 Objectives

2.1 Objectives

The objective of the present study is to investigate one of the main physical channel-shoal interaction mechanisms: (i) the interaction between turbulence and concentration on intertidal areas, which might lead to sediment-induced density current and (ii) the supposed collapse of the turbulence field and concentration profile when the saturation concentration is exceeded.

2.2 Methods and approach

Two important tools were planned used in the first part of this R&D project: simulations with computer codes and an analysis of field measurements. Not all these tools have been used in the project however. First the anticipated use of the tools is described, than the reason why they were (not) used is treated.

2.2.1 Model simulations

First, computer codes describing the total turbulence – sediment concentration interaction in a one-dimensional vertical approach were planned to be used. One of the codes, a 1-DV model, has been developed in recent years at Delft Hydraulics and is known as the 1DV Point Model. This model has in fact been obtained from DELFT3D by stripping all horizontal transport components and adding various sediment modules (e.g. a flocculation model). It was planned to use it as the primary theoretical analysis tool. Also Delft3D with the implementation of sediment-fluid interactions, see Lesser et al. (2003), was planned to be used.

2.2.2 Data analysis

Second, this project has access to a large intertidal area data set from a measurement campaign performed at the Paulina salt marsh in the WesterScheldt from June 11th 2002 to October 12th 2002. This data set was primarily set up to investigate the influence of vegetation on hydrodynamic parameters. The aim of this study is well formulated in Bouma et al. 2003, a few useful paragraphs of which are enclosed in Appendix A. Four frames have been used in this campaign (RIZA1/2, AMF, DON). Only one of these frames (the DON-frame) measured data at two levels, the others measured only at one level. Only the data from the DON-frame are used in this project.

During the 2002-Paulina campaign, the DON frame recorded velocities at 7 and 15 cm from the bottom and turbidities at 15 and 25 cm from the bottom (Figure 1). Also the water level was measured, which ranged from zero (the flat was dry during ebb) to 2.5 meters during spring tide. The data have been collected at 4 Hz with 8 minutes burst interspersed with 7 minute breaks. The data from this campaign are referred to as the low-frequency data

from now on. For details on the set-up of the frame, the calibration of the data or the processing, see annex B.

As a part of the long term campaign mentioned above an additional short (2 day) mini campaign has been undertaken. This mini-campaign specifically aimed at measuring the interaction between turbulence characteristics and SPM values. These data were collected at 16 Hz divided in two full 8 hour bursts, each covering one whole tide. The same frame with the same equipment was used as with the 4 Hz data. These data are suitable for studying the interaction between the vertical turbulence and concentration profiles as described in Van der Ham [1999] and Winterwerp [1999]. Before the measurement campaign started, a bottle sample was taken at the edge of the flat, showing a concentration of over 300 mg/l. This high value gave confidence that the expected trapping effect would indeed occur. The data from this campaign are referred to as the high-frequency data from now on.

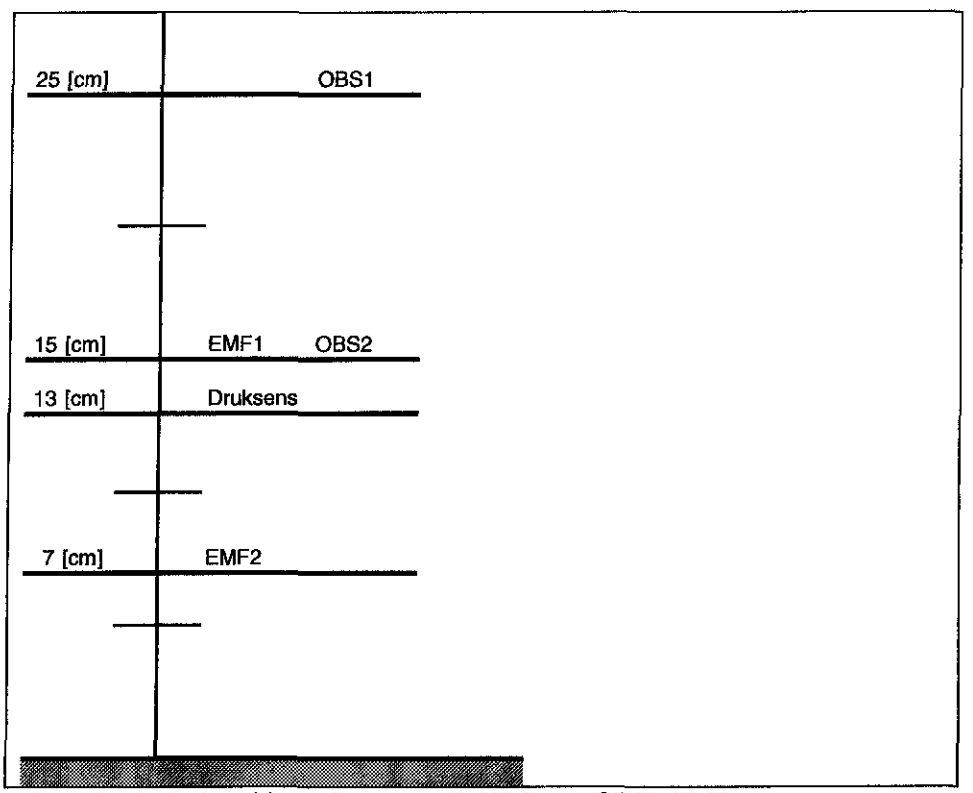

Figure 1. Vertical position of sensors at DON frame. OBS1,OBS2 = sensors measuring respectively sediment concentrations ftu_1 and ftu_1, EMF1, EMF2 = velocity sensors measuring respectively (v_{x1}, v_{y1}) and (v_{x2}, v_{y2}), where $_{x, y}$ refer to the x and y-direction, druksens = water level sensor.

2.2.3 Original approach

The original approach of the present study was as follows:

The feed-back between turbulence and sediment concentration, leading to the turbulence collapse sediment trapping mechanism on shallow areas, will be investigated by means of

a) Analysing the 2 day 16 Hz data set obtained at one point on the intertidal flat by plotting time series and power spectra.
b) Model simulations with an advanced one dimensional vertical model (1DV Point Model) using the analysed high frequency data

c) Analysing a 100 day 4 Hz data set by plotting time series.
d) 2DH and 3D model simulations for entire intertidal flat using the analysed low-frequency data

The boundary conditions for the turbulence profile imposed by means of the bottom roughness

a) Simulations with 2DV-3D Delft3D online-sed model
b) Implementation and testing of bottom roughness boundary condition by Toorman [1999] for turbulence in 1DV Point Model.

Studying the effect of model assumptions on the combined effect of grid size and bed roughness

2.2.4 Final approach

The priority of addressing the various sub-topics was as follows: the research project started with the first topic described above, and would pay attention to each successive step if the previous step would be dealt with sufficiently. However, due to some setbacks and unexpected results not all of these steps have been accomplished. In fact only step 1a and 1 c have been performed.

2.2.4.1 Data analysis

The 4 Hz-data and the 16 Hz-data have been analysed. The analysis of the field measurements took much longer than expected though. The underlying reasons for this are

- A loss of all processed data due to a mistake of the computer department. This required a time-consuming re-processing of all data.
- The need for a time-consuming extra calibration *post hoc* of the sediment concentration data
- The time needed for writing post-processing scripts was underestimated.

2.2.4.2 Model simulations

The model simulations have not been performed at all, since the nature of the field data did not allow adequate simulations to be performed. The underlying reasons for this were (i) the fact that velocity data showed a veering with height and (ii) that the quality of the sediment data were insufficient to set-up sediment concentration profiles. The 1-DV model needs the average velocity as input. But due to the veering of the velocity, it was not possible to extract the average velocity from the data by fitting a velocity profile. Therefore the 1DV model was not considered adequate any more. The DELFT3D simulations have not been performed at all. These were too time consuming and could not be performed any more in the remaining time as the data analysis took more time than anticipated. It is recommended to perform these 3D simulations in the future.

3 Results

3.1.1 Analysis of high frequency data

In the first part of this project a thorough analysis of the two days of 16 Hz measurements has been performed. The measured time series of the velocity, turbidity and water level during day 255 and 256 of 2002 are shown in Figure 2. Furthermore, the time series of the 4 velocity components have been analysed by calculating the power spectra over 11 minute intervals, one example of which is shown in Figure 3 and 4. As one can see in figures 2 to 4, the expected collapse of the turbulence field does not occur: (i) the fluctuations in the velocity signal, a measure of the turbulence, do not disappear, (ii) we do not see a sudden, strong decay in the concentration profile. One hypothesis for this is that the concentrations at the site were too low (10-100 mg/l) for a sediment-induced collapse of the turbulence profile. The concentrations are still high enough for sediment-flow interaction though, for sediment-induced density currents play a role at sediment concentrations as low as 100 mg/l (Winterwerp and Van Kessel, 2002). However, the concentration data are not adequate to say something about the concentration profile (vertical gradients), as is explained below.

According to plan, in the second part of this project the feed-back of sediment-induced density on turbulence would be investigated by means of simulations with a 1DV numerical model. Simulations would be performed to indicate under what circumstances the collapse might have occurred, and also why it didn't occur during the measurements. However, due to two setbacks it is not possible to model such a measured collapse.

The first reason is that on one data stream of the velocity sensor (v_{x1}) an erroneous offset is discerned due to which the average velocity (direction and amplitude) cannot be determined. Since the 1DV model needs the average velocity as input, the simulations cannot be performed. The fact that an offset was introduced was not discovered until analysing the long time-series of low-frequency (4 Hz) data performed hereafter, which did not show this offset. After some research it was concluded that most probably only an artificial offset in one sensor in one direction was introduced (viz. v_{x1}). This means that the turbulence characteristics are not influenced by this offset and are still correct. The spectral data in Figure 3 are therefore still correct.

The concentration (turbidity) profiles show higher concentrations near the surface (at 25 cm) than near the bed (at 15 cm) (see Figure 1). After a reanalysis of the measurements, it turned out that the calibration of the OBS sensors was not performed adequately at the time the data were collected. Even after a thorough recalibration of the OBS sensors with an original mud bed sample (see annex B), this fact remained. It should be noted though that the difference is only 5 mg/l on an average signal in the order of 50 mg/l. This has a major implication though.

When the OBS data are used in a quantitative sense, an error of 10% should be taken into account. Since this error is too large for inter-comparison of the OBS data at two levels, it is not possible to get spatial information (information about vertical sediment gradients) from the OBS data. Therefore the data cannot be used for the purpose we anticipated: measuring vertical gradients. This lack of spatial information is the second reason that the 1-DV model runs cannot be performed (besides the offset in one velocity component mentioned above).

It should be noted that the individual recalibrated OBS data are still valuable, and still more valuable than one single OBS registration. Events affecting the vertical distribution of sediment can still be analysed in an qualitative way, albeit in an indirect manner. One method is to assess the delay of events recorded at a higher level (if the event reaches that level at all, which is also very useful information). A second method is to use the relative amplitude of events with respect to the mean signal.

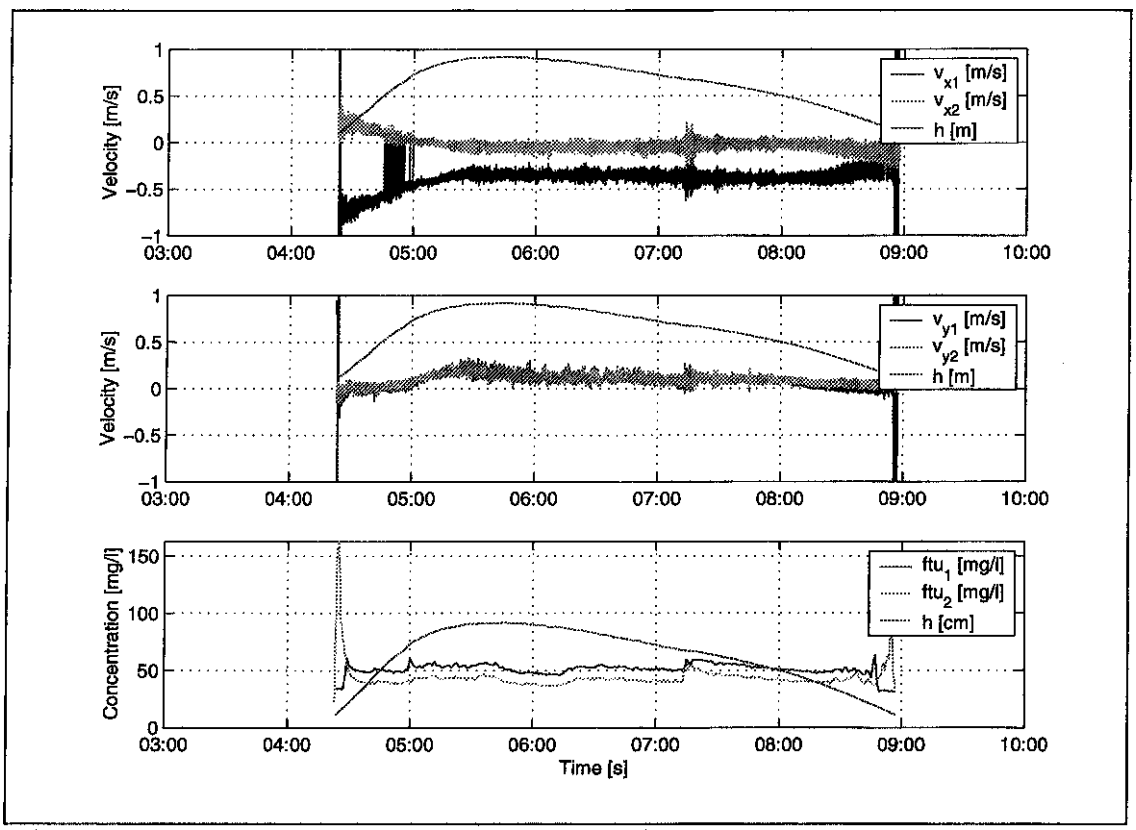

Figure 2 a: Time series of 16 Hz data recorded at day 255, 2002. Shown are registration of the x and y velocities $v_{x/y1}$ (15 cm), $v_{x/y2}$ (7 cm), the concentrations ftu_1 (25 cm), ftu_2 (15 cm) and water level h (see Figure 1). (Note: v_{x1} is plotted as $-v_{x1}$). Note the presence of waves and the sudden ripples in the concentrations at 7:20 on day 255 and 6:10 on day 256. Note also the offset in vx1 of about 0.4 m/s. Note also that the concentrations at height 1 (25 cm) are higher than at height 2 (15 cm)

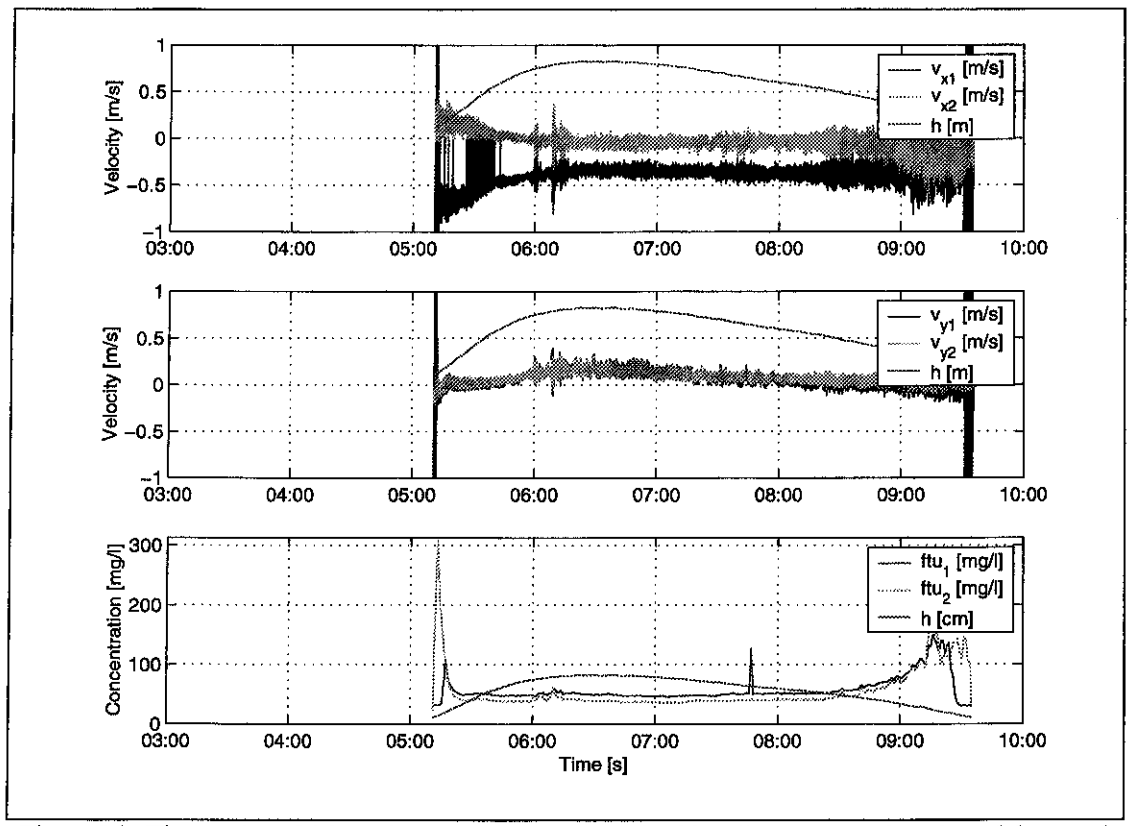

Figure 2 b: Time series of 16 Hz data recorded at day 256, 2002. Shown are registration of the x and y velocities $v_{x/y1}$ (15 cm), $v_{x/y2}$ (7 cm), the concentrations ftu_1 (25 cm), ftu_2 (15 cm) and water level h (see Figure 1). (Note: v_{x1} is plotted as $-v_{x1}$). Note the presence of waves and the sudden ripples in the concentrations at 7:20 on day 255 and 6:10 on day 256. Note also the offset in vx1 of about 0.4 m/s. Note also that the concentrations at height 1 (25 cm) are higher than at height 2 (15 cm)

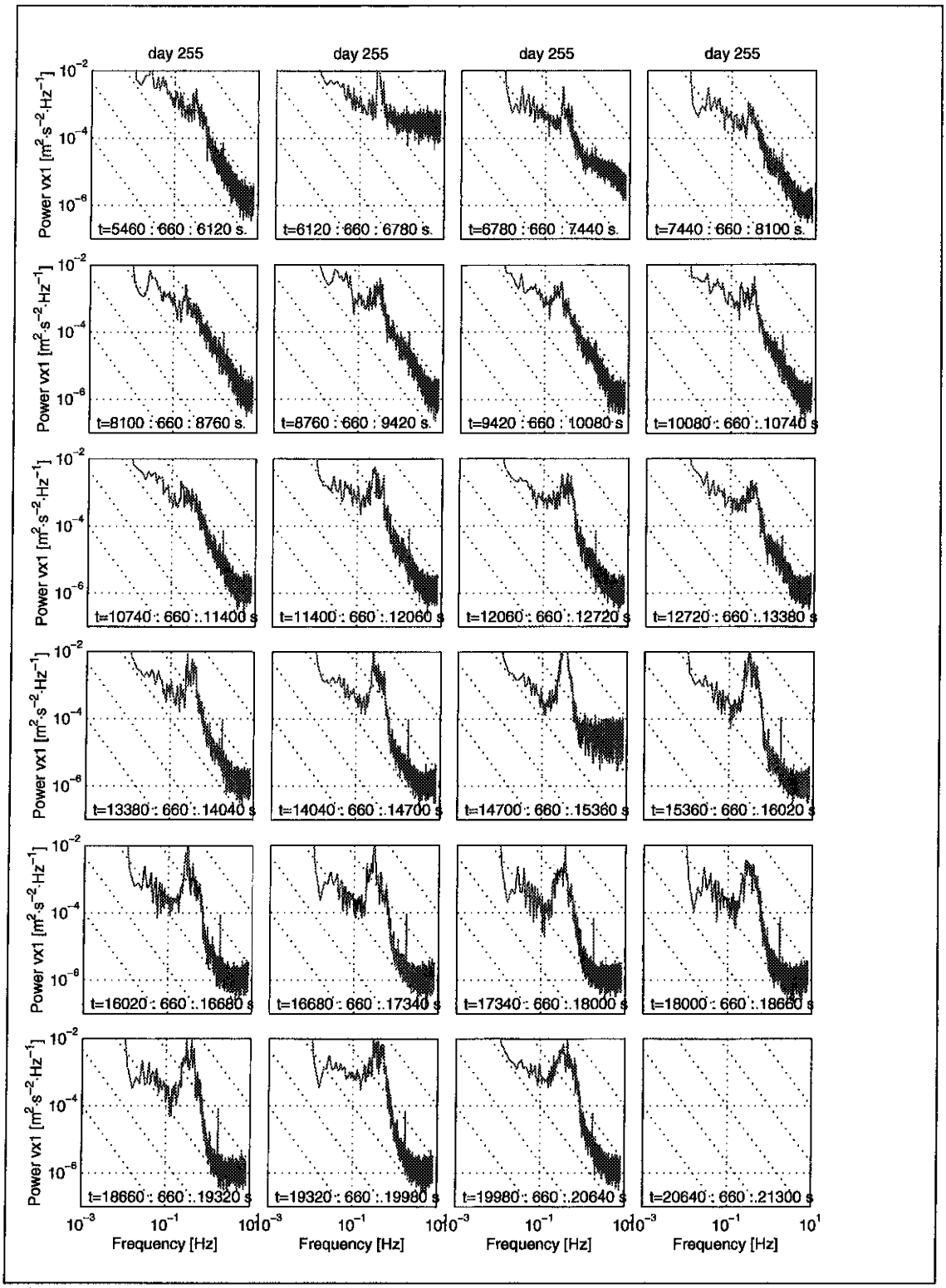

Figure 3: Power spectra over 11 minutes of 16 Hz velocities data recorded at height 1 (15 cm) in x-direction at day 255, 2002 (v_{x1}). Note the strong wave peaks at about 0.3 Hz (~3 sec.). Note also the strong presence of waves with t~3 s at t=14700 s (peak outreaching max axes value). The spectrum at t=6120 (box 2) s is wrong as can be seen the associated time series in the next figure. For background details of this spectrum see appendix B.8. The dotted lines at a 36/60° angle indicate the 5/3-turbulence law: in turbulence the signal power generally decreases with increasing frequency with this slope.

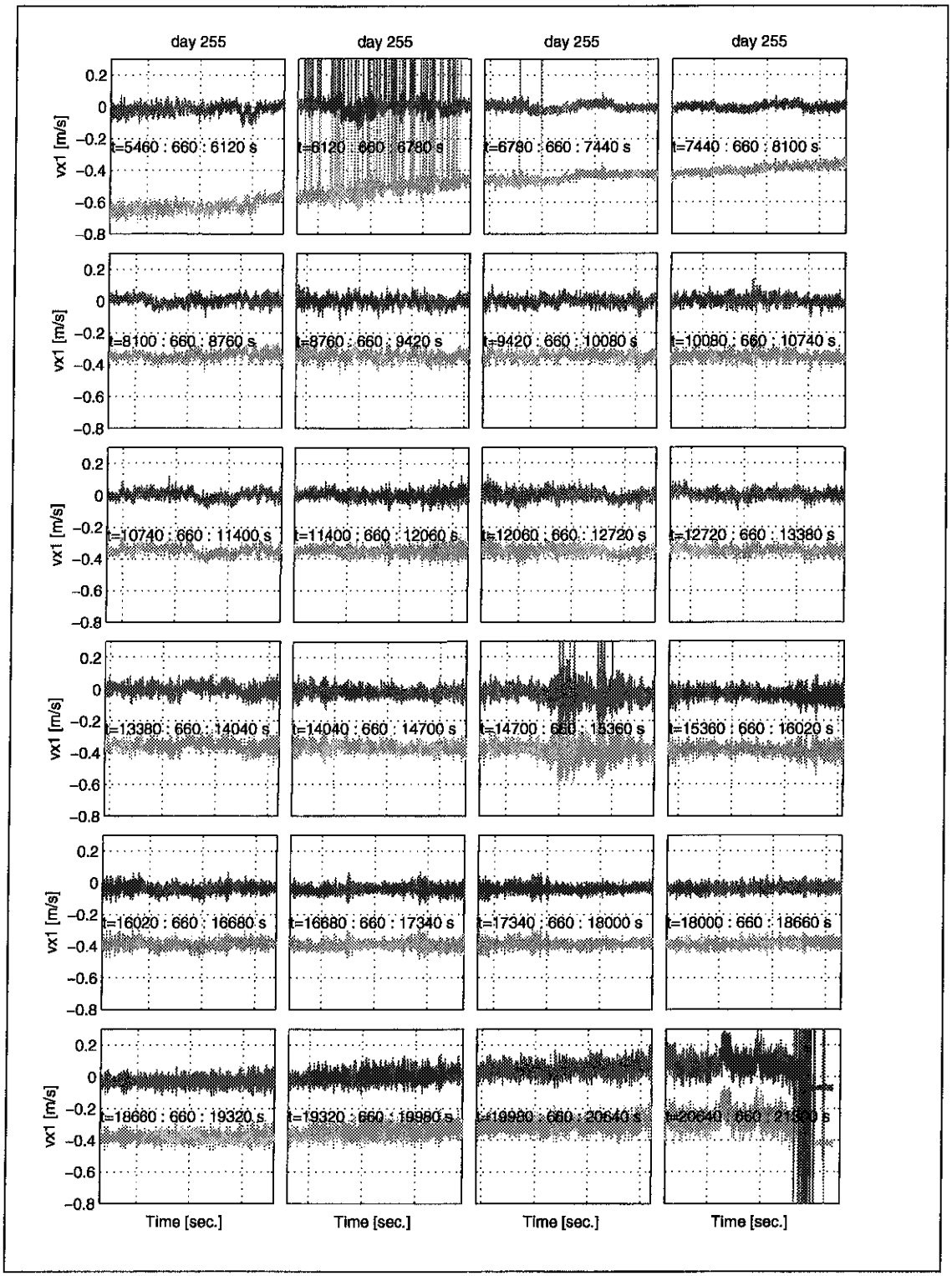

Figure 4: Times series of 16 Hz velocities data recorded at height 1 (15 cm) in x-direction at day 255, 2002 (v_{x1}). Shown are the actual signal (pink, dark) and the residual signal (cyan, light) when the mean per 11 minute box is removed from the measured signal. Each time series box corresponds to the power spectrum box at the same position in the previous figure. Note the artificial offset in the velocities of about 0.4 m/s which is not present in any day of the 100-day low-frequency data set. Note also the presence of (ship) waves at t=14700 s.

Despite the setbacks in the measurements, some unexpected, but very interesting phenomena worth studying are observed in the data.

- The turbulence measurements show a strong oscillations with a 3 to 6 second period in the spectral plots of the turbulence data at all times (see Figure 3 and 4). This indicates the presence of wind waves. Usually it is assumed that the presence of waves leads to high concentrations. Generally the concentrations on tidal are flats are indeed high most of the time, but during this measurement the concentrations were only 50 mg/l on average and did not exceed 160 mg/l.

- A few small periods in the total data series exhibited an unusual strong wave group signal (See 7:20 on day 255 and 6:10 on day 256 in Figure 2 and also t=14700 in Figure 3 and 4). This is probably a wave train originating from a passing ship. The concentrations immediately after this event show a significant increase (sudden increase of 20-30 %). There are two possible explanations for this: either it implies that the bed contains a layer of very fluffy freshly deposited material that is locally resuspended or it implies that the material is entrained closer to the main channel and advected onshore. The time lag between the passing of the ship waves and the concentration 'jump' might give more information on this matter (Figure 5 and 6). On day 255 (Figure 5) the ship wave does not have a clear beginning. We can clearly see though that the concentration increases suddenly by about 10 mg/l after 1 a 2 minutes. When we take into account the fact that the water speed is order 0.1m/s, the sediment cannot be advected from more than about 10 m distance. We also see that the bottom concentration (*ftu*2) increases before *ftu*1, indicating local resuspension (as the bottom velocity v2 is nearly equal to v1, and taking into account the 0.4 m/s offset, it cannot be a density current). We can estimate the time needed for the sediment to reach the sensors. This time is proportional to the height squared divided by the mixing coefficient: $T \sim h^2/\varepsilon$. When we assume as a first guess $\varepsilon = 0.1 \cdot h \cdot u_*$, and assume u_* to be about 0.05 m/s (half the standard deviation of the velocity signal at 7 cm) we get a time scale of 1 minute. However, the sampling rate of the concentration measurements is only 1 minute (1/60 Hz), which is about equal to the time lag. This means that we cannot easily discern the difference between local advection and re-entrainment right underneath the DON frame from this event. We can conclude though that sediment is resuspended somewhere close to the DON frame (but not necessarily right underneath the DON frame). The same analysis applies for the event at day 256 (Figure 6). Contrary to Figure 5, here onset of the ship wave is clearly visible, but the increase in concentration is not less clear. The concentration here also increases after about 2 minutes after the onset of the ship wave (between 135-136).

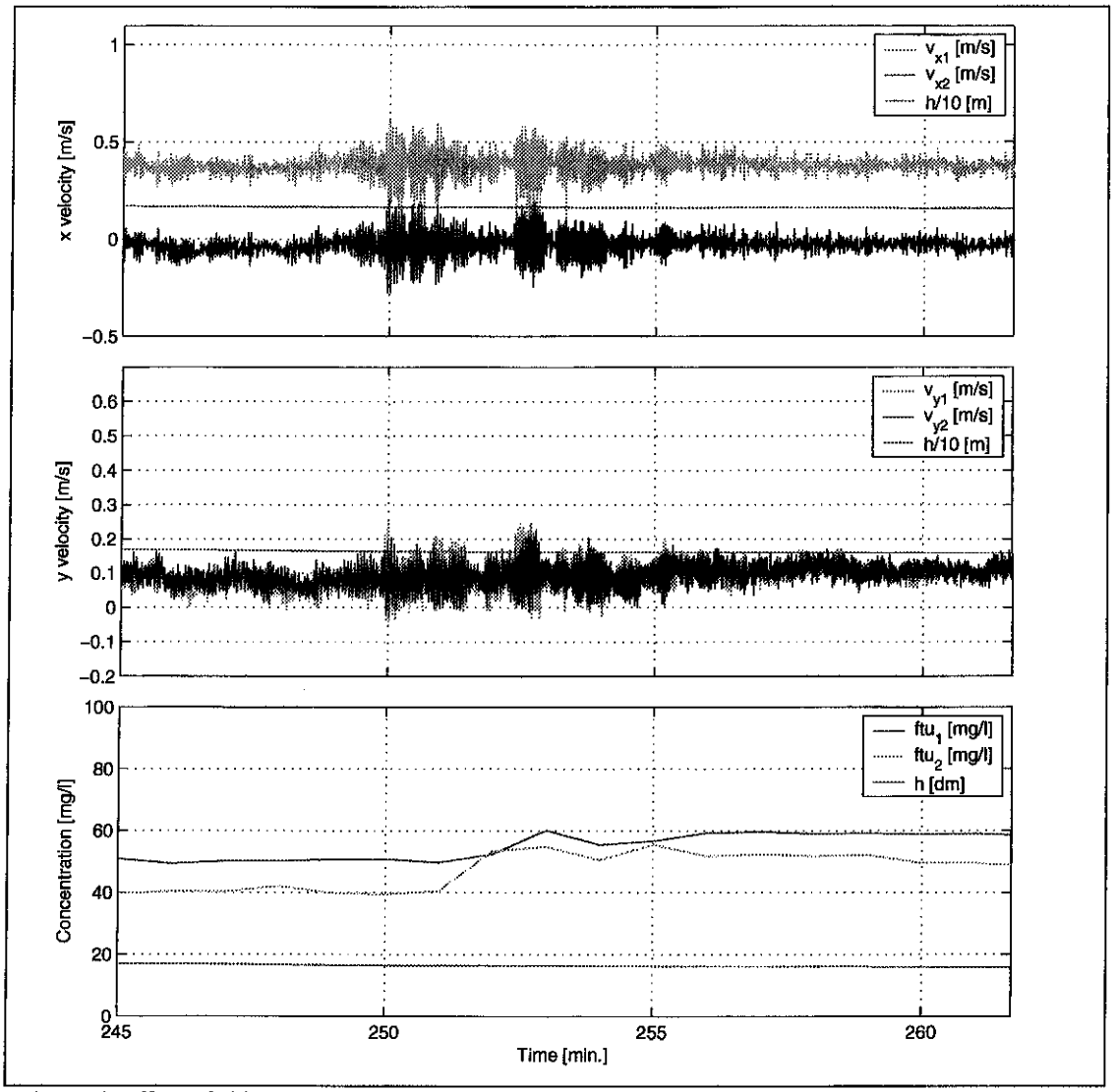

Figure 5: Effect of ship waves on concentration on day 255 at about 7:20.

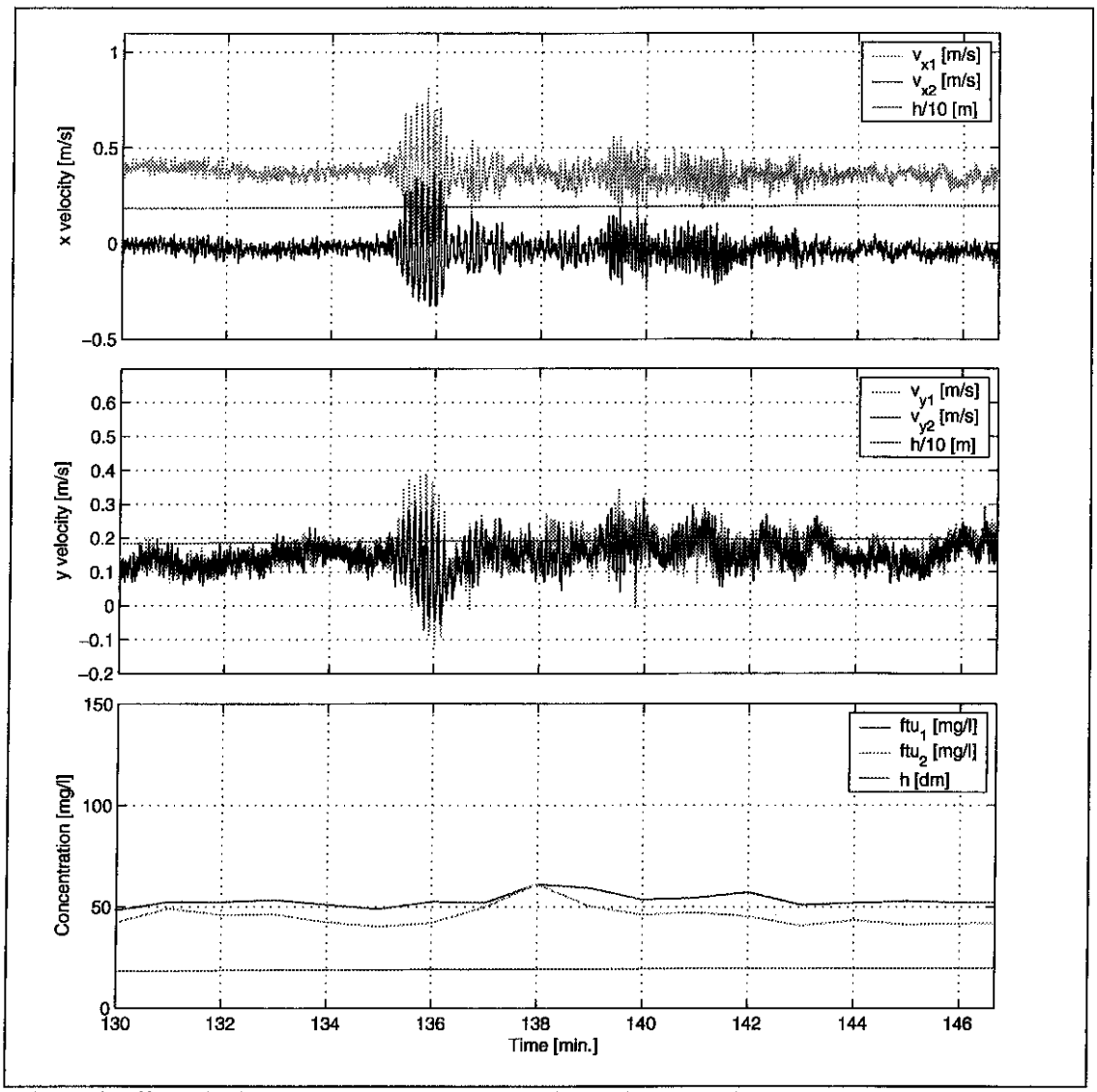

Figure 6: Effect of ship waves on concentration on day 256 at about 6:10.

3.1.2 Analysis of low frequency data

The collapse of turbulence and concentration profiles did not occur in the two days of high-frequency data, nor could this phenomenon be modelled with the 1DV model. Also the presence of sediment-fluid interaction (density currents) could not be detected from the data. Therefore, the complete 100-day set of low frequency data was analysed in search for sediment-fluid interaction, and the supposed collapse of the concentration profile. It should be noted that this data set had already been analysed in a previous project. However, those analyses did only concern the time-averaged data, and did not take a look at the raw, underlying 4 Hz data. The result from the reanalysis is:

- During the approximately 100 days of low-frequency data, the collapse of the turbulence and concentration profiles did not occur either. The time-series do not show that (i) the fluctuations in the velocity signal (a measure of the turbulence) suddenly disappear, (ii) or a sudden, strong decay in the concentration profile.

- The velocity data do not show the erroneous offset as observed in the 16 Hz data, except for the last few days (which were in fact recorded just before the 16 Hz measurements were collected). This means that the data can, at least in principle, be used to calculate the average velocity, and can accordingly be used as input for the 1DV model.
- The velocity data exhibit the characteristic and expected behaviour of the larger scale hydrodynamics. The marsh floods with velocities directed almost cross-shore, albeit most times with a small upstream component (w.r.t. the WesterScheldt). During rising of the water level the velocity vectors gradually rotate anti-clockwise and become directed almost alongshore. During ebbing the velocities turn anti-clockwise even more and become directed towards the main channel, with a small downstream component (Fig 7).
- The average velocity amplitudes and directions show a large variability from day to day, probably due to wind and, to a lesser extent, waves (Figure 8). This means that the local transport, erosion and deposition characteristics, which are very closely related to the velocities, are also very variable. The momentum transfer from the wind is indeed expected to have a large influence on the water motion on the march. The water depth on the flat is small, especially when it is not high water. Accordingly, the total mass of the water column is small and the momentum transfer from the wind to the small water mass (per unit area) will therefore have a large affect. The day-to-day velocity variations can therefore likely be attributed to the wind.
- Wind forcing acts as an additional source of turbulent energy, besides bottom friction. In the supposed collapse of the concentration profile, it is assumed that the bottom-generated turbulence cannot penetrate into the water column any more, thereby reducing the carrying capacity of the flow. When wind generates additional turbulence at the water surface, it can prevent the supposed collapse of the concentration and turbulence profiles.

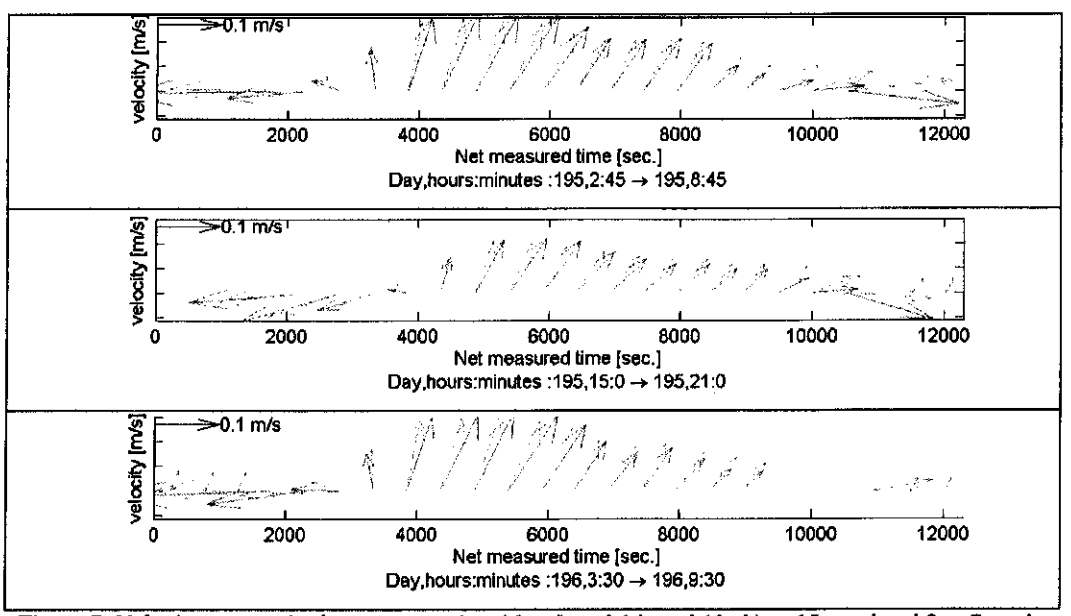

Figure 7: Velocity vectors in three consecutive tides. Level 1 in red (dark) at 15 cm, level 2 at 7 cm in green (light). X-direction points to Borssele, y-direction points 90 degrees east of x. Note i) the veering with height at the end of the tide and ii) that the strongest velocities occur during ebbing and flooding. (Do not pay attention to the missing vectors due to corrupt data or to the artefacts such as the first 3 small arrows in third panel).

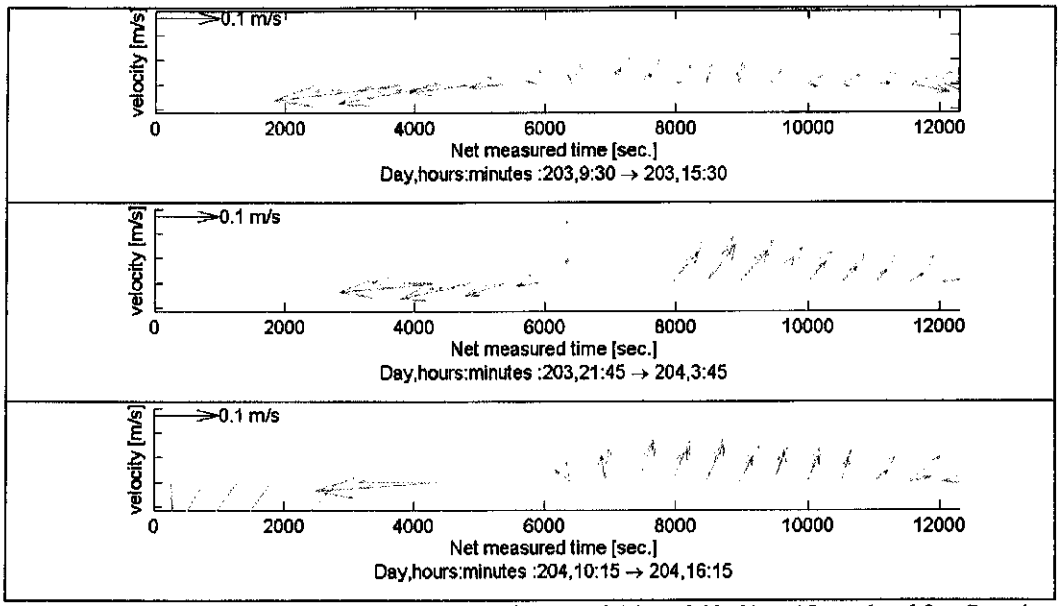

Figure 8: Velocity vectors in three consecutive tides. Level 1 in red (dark) at 15 cm, level 2 at 7 cm in green (light). X-direction points to Borssele, y-direction points 90 degrees east of x. Note i) the strong day to day variability in the velocities and ii) the fact that during these days of low velocities (just after neap tide) the near bottom velocities (green, light) are higher than the overlying velocities (red, dark) during almost during the entire tide (except for flooding) and iii) the veering with height during ebbing, but also during high water when the velocities are low (first panel). (Do not pay attention to the missing vectors due to corrupt data or to the artefacts such as the first extraordinarily long arrows in third panel).

- During high water, the velocities are a little more than 10 cm/s, while the standard deviation is of the same order. This implies that the turbulence (due to waves) has a large influence on the bottom shear stress, even larger than the bed shear stress due to the mean current.

- During high water the velocities at the two levels are almost parallel, with the near-bottom velocity being smaller almost all of the time. This phase of the tide can probably well be described by fitting a log profile.

- During ebbing and flooding the velocities are higher than during high water, almost 20 cm/s, while during high water the velocities just exceed 10 cm/s. This means that the water has to decelerate towards high water and to accelerate afterwards. Consequently, during these periods the velocity profile cannot be described with a log profile. A log profile is not valid for accelerating and decelerating tide.

- Moreover, during ebbing and flooding a completely different current situation arises: the velocity data show a veering with height (last arrows in first 2 panels in Figure 7). This might indicate the presence of density currents and hence the presence of sediment-fluid interaction (without necessarily a collapse of the concentration profile). This veering can be explained as follows: generally the heavier density current near the bottom will be guided by local topography, while the water motion in the rest of the column is driven by the large scale effects as and the tidal propagation in the main channel. Another

explanation of the veering with height might be presence of wind. However, when the veering occurs, it is almost always in the same direction. The most likely explanation for this is the presence of density currents, guided by local topography. It might also indicate a dominance of one direction in the wind climate though, although this hypothesis is less likely. It should be noted that Johan de Kok of RIKZ mentioned that this veering might be also caused by Coriolis. Generally Coriolis effects do not play a role at spatial scales this small. Moreover, the velocities are small (order 10 cm/s). Since the Coriolis effect is proportional to the velocity, this effect is expected to be small. But it is true that when density currents are present, Coriolis effects become more important. This aspect needs further investigation.

- The veering of the velocity with height, and accordingly the density current associated with this, are mainly visible during the ebbing and flooding of the mars. Sometimes, when the velocities are low (neap tide) the veering is also observed during high water (first panel of Figure 8). An important note is also that that when the veering is most clearly visible in Figure 7 (last arrows in first 2 panels in Figure 7), the velocities have their maximum values. This would obviously not be in agreement with the fulfilment of the saturation criterion u_*^3/h, so we can be sure that a collapse did not occur during these periods. The saturation concentration u_*^3/h is most likely exceeded when the velocities are low, which is not during the beginning and end of immersion (the ebb and flood 'bores'). This observation is not in agreement with the hypothesis mentioned in section 1.3 that the collapse would most likely occur during ebbing and flooding. The hypothesis has to be amended in the sense that the ebb and flood bore are excluded. A corroboration of the hypothesis that the density current was the result of a sediment-flow interaction, is that this density current mainly occurred when *after* the velocities were low, i.e. during neap tide, and during the first part of ebbing.

- The veering of the velocity with height over only 7 centimetres also says something about the eddy viscosity of the water: the eddy should be quite low to allow such a string local shear to persist. This low eddy viscosity is another indication that the sediment concentration on the marsh is high and that sediment-fluid interaction is going on.

- The veering of the velocity with height has a few implications:
  - It is not possible, nor does it make any sense, to fit a velocity profile (Van Veen, Log, etc.) to the data during ebbing and flooding. This means that information about the average velocity cannot be extracted from the data.
  - If the average velocity cannot be extracted from the data, it is not possible make model simulations with the 1-DV model, which requires the average velocity as input.
  - Note that 1DV modelling of the feed-back between turbulence and sediment concentration of the data still makes sense if there is a veering of velocity with height, since the 1DV model does not take into account any directional information. The fact that a density current near the bed would have another direction than the main current is not taken into account, only the magnitudes matter. Comparing model results to vertically veered data will require some additional interpretation steps though.

- For determining the average velocity on the location of the DON-frame, 3D model simulations are required. It should be noted that useful model simulations with a 3D model, i.e. including the veering of the velocity on the salt marsh, will be dependent on the presence of feed-back of concentrations on the density in the model. This feed-back is present in Delft3D. For studying the influence of concentration gradients which are not due to turbulence-density interaction on the current, this is a promising approach. Performing 3D model simulations in order to gather input for a 1DV model is a bit the other way around though. If 3D model runs are performed anyhow, it is more sensible to study the feed-back phenomenon with the 3D model itself. A few warnings should be made concerning this approach though:
  - Modelling the salt marsh with a sufficiently fine resolution with Delft3D might lead to very long calculation times. The fine vertical resolution which is probably required for this 3D modelling, will even increase calculation times even further.
  - The wetting and drying of cells on the salt marsh might be troublesome when modelling concentrations and using sigma layers. The choice for the minimum water level in a dry grid cell has a large influence on the maximum concentrations just after wetting or before drying. As we can see in the DON-data (Figure 2), the highest concentrations occur in these very periods. For studying the feed-back of concentration on turbulence these very concentrations are of paramount importance.
  - When wind forcing is included in the simulations, a set-up of the average water level over the entire intertidal area has to be taken into account. This set-up has to be accounted for in the boundary conditions

- The highest concentrations occur during ebbing and flooding, while the highest velocities also occur during ebbing and flooding. Moreover, the highest turbulence (standard deviation of the velocities) is also found during these phases and hence the carrying capacity is highest in this period. This means the majority of the onshore and offshore transport occurs during the initial and final phase of the flooding of the marsh. The net sedimentation and erosion of the march will therefore be governed by the difference between these two large onshore and offshore fluxes. This fact has also been recognized by Christie et al. 1999:

> "The integration of the sediment flux over time and water depth defines the water column suspended sediment transport rate (q_s), and in this respect, the sediment flux is analogous to the transport rate. The transport rate (q_s) was calculated, being equal to the integral through depth of the depth mean velocity and concentration values, assuming a logarithmic velocity profile and homogeneous concentration profile. A residual transport rate R_f was calculated in a similar fashion. However, q_s depends upon accurate descriptions of the vertical velocity and concentration profiles, and it is impossible to precisely quantify q_s using measurements from one height above the bed.
>
> "The variations in the velocity and concentration data produced a cross-shore dominated, suspended sedimented flux. Longshore components of the sediment flux were extremely small and occurred around high water when concentrations were generally low. R_f units were kg m^{-2} $tide^{-1}$, being the difference between the total integrated flux during the flood period and the integrated ebb value, where the transition between flood to ebb phase was defined by the maximum water depth (h_{max}). The residual flux direction was thus landward or seaward, with a positive residual flux denoting onshore transport. The R_f value was often the small difference between two relatively large numbers and errors in the raw data could

significantly affect the residual flux value, and even alter its direction. *Maximum flux values occurred in the shallows (< 0.5 deep, at the beginning and end of immersion), when concentrations and velocities were large.* However, instrument errors were potentially greatest at this time (because of wave splash and wetting effects) and so the first and last data points were rejected."

The assumptions made by Christie et al. 1999 to calculate the net on-offshore sediment flux are not considered applicable to the Paulina marsh data. In the Paulina data the velocities have been measured at two levels, and from these data we can conclude that we cannot fit a (logarithmic) velocity profile to the (veering) data. Model simulations with Delft3D are necessary to calculate the cross shore and alongshore fluxes.

- The (ship) waves, which were present in the high-frequency data, are also present in the low-frequency data. See Figure 9 to 11 below for a nice example in three zoom levels. The time lag between the onset of the ship waves and the increase in concentration is about 150 seconds. The same analysis applies as to the ship waves in the 16 Hz data: the sediment is resuspended locally, but not necessarily directly underneath the DON-frame.

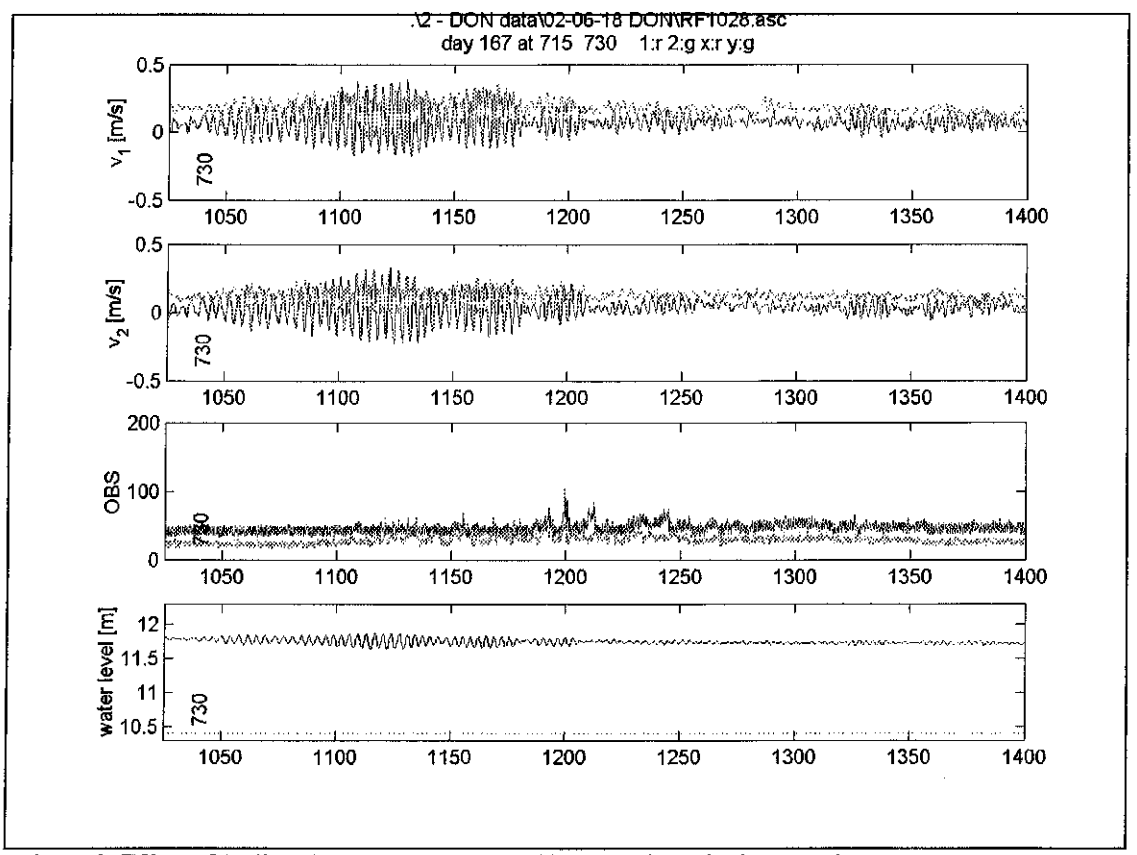

Figure 9. Effect of 'solitary' wave group on a ~ 400 seconds = 6 minute scale.

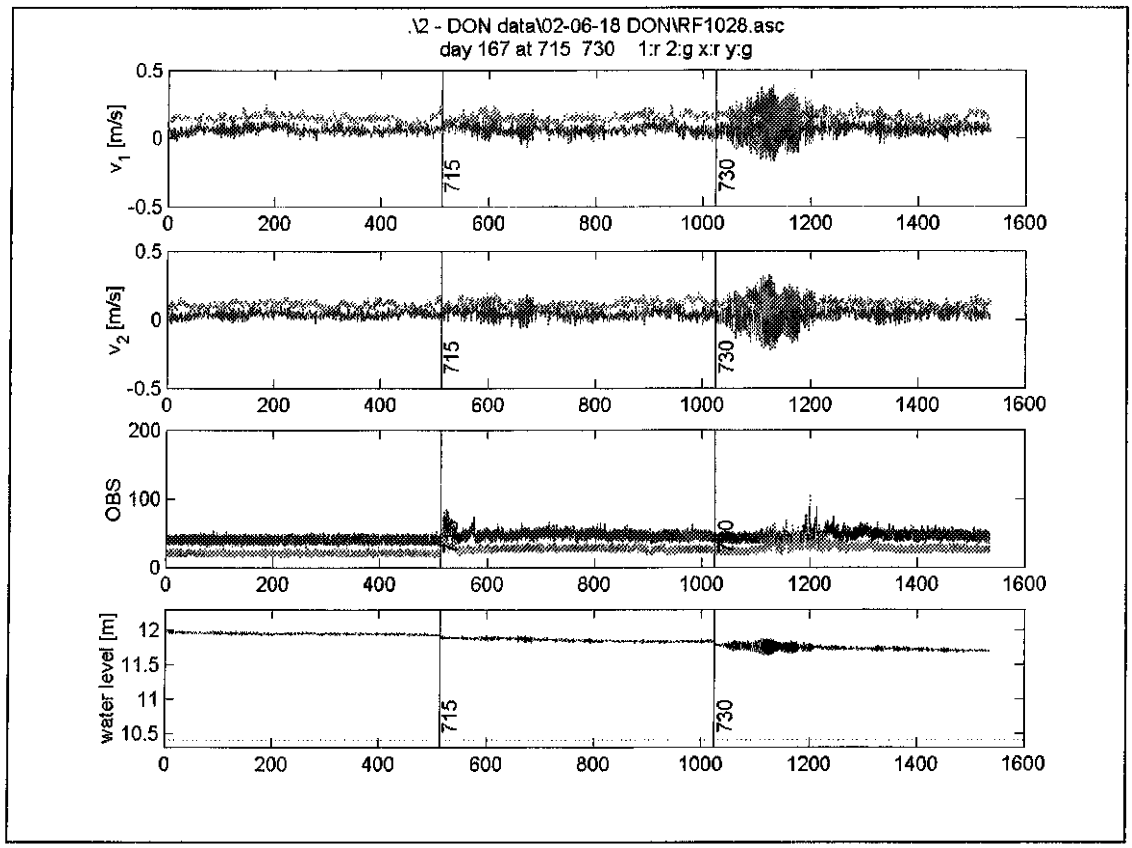

Figure 10. Effect of 'solitary' wave group on a 15 min scale.

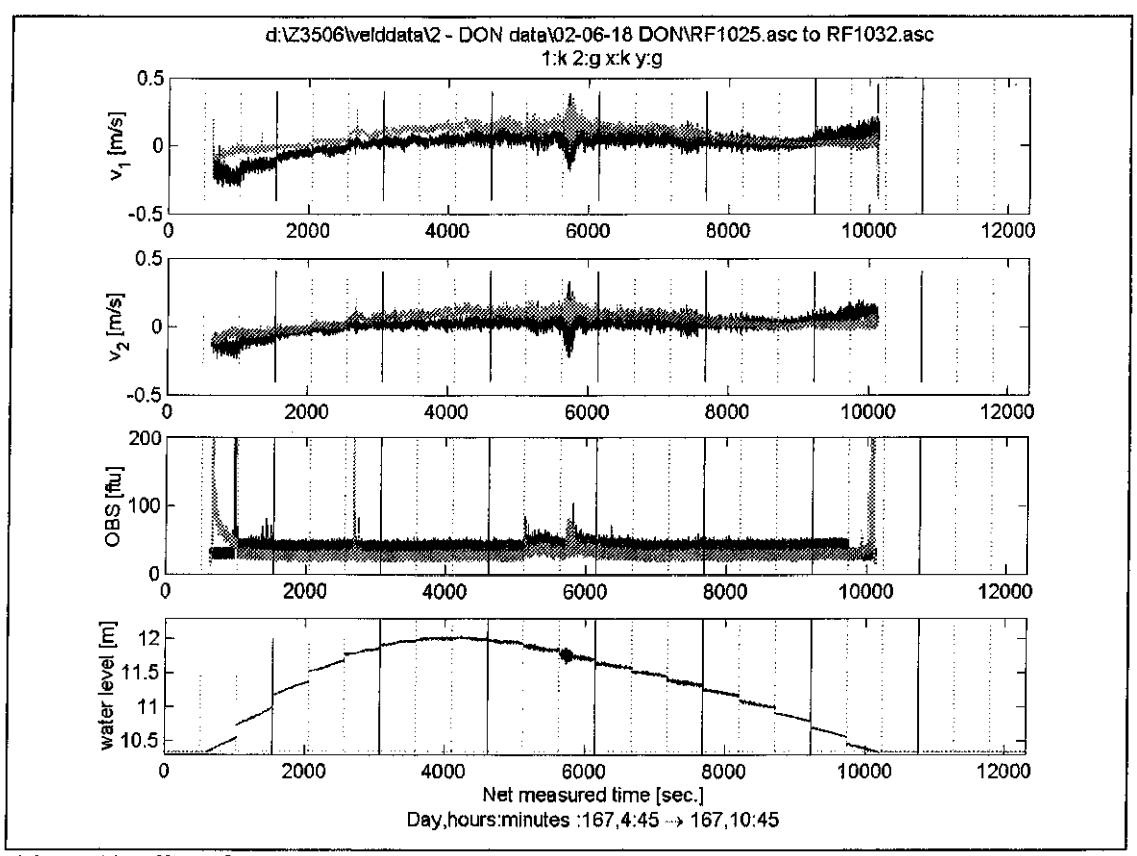

Figure 11. Effect of 'solitary' wave group on a full tidal scale.

4 Discussion, summary and recommendations

4.1 Summary

4.1.1 Introduction

The area of intertidal areas in the Netherlands has tremendously decreased over the last decades. For management of the remaining area of inter tidal areas, knowledge of (i) the sediment fluxes into these basins, (ii) their net accumulation within these basins as well as (iii) their distribution over these basins is indispensable. However, we do not really understand yet how intertidal areas catch fine sediment. A few processes are (expected to be) responsible for catching fine sediment on intertidal areas. One of these processes is the interaction between turbulence and sediment induced buoyancy effects. The objective of the present study was to investigate: (i) the interaction between turbulence and sediment concentration on intertidal areas, which might lead to sediment-induced density currents and (ii) the possible collapse of the turbulence field and concentration profile when the saturation concentration is exceeded. The original approach of this project was to investigate this feed-back mechanism by (i) data analysis and (ii) model studies. Due to some setbacks only the data analysis has been performed.

4.1.2 Data analysis

The data analysis concerned velocity, turbidity and water level measurements at the Paulina intertidal area in the WesterScheldt. 4 Hz data were collected for about 100 days in the summer of 2002, followed by 2 days of 16 Hz data in October. The velocity and turbidity data were collected at two levels. This allows one to say something about vertical gradients.

First, when the supposed collapse would occur, this would be visible in a sudden decrease of the entire concentration profile and of the turbulent fluctuations. However, inspection of all the data showed that the collapse did not occur. Possibly the concentrations were too low for this effect to occur.

Second, the (generation of) density currents would be visible in the vertical concentration gradients. Unfortunately, due to an inadequate calibration of the turbidity sensors, the concentration values near the bed are larger than the ones higher in the water column. This makes it impossible to say anything about vertical gradients in the concentration profile from the data. However, another phenomenon may indicate the presence of sediment-induced effects: many velocities recordings show a 10 to 30 degree veering with height, possibly indicating the presence of a density current. The hypothesis is that a bottom density current is formed by the interaction between turbulence and sediment concentration. This under-current is then directed by local topography, while the higher layer is governed by larger scale hydrodynamic features. The fact that such a large shear is able to persist for a longer time over such a small distance (7 cm), might also suggest that strong sediment-fluid interactions are present, damping out the eddy viscosity, which would otherwise disturb the veering of the velocity with height. However, the veering may also be the result of wind and/or Coriolis effects. This aspect needs further investigation.

A further corroboration of the hypothesis that the density current is the result of sediment–flow interaction, is that this density current mainly occurs *after* the velocities are low, i.e. during neap tide and during first part of ebbing. Thus, although the expected density currents were not observed directly, an indirect clue to their presence has been found. It is recommended to focus further research on this observation.

A second important phenomenon has also been observed in the Pauline data. The sediment concentrations, the velocities and the turbulence on the tidal flat are highest at the beginning and end of immersion of the tidal flat. As the sediment fluxes are calculated by multiplying the concentration with velocities, the transports are also expected to be highest at the beginning and end of immersion. This means that to assess whether a tidal flat catches sediment or not, one has to subtract a large offshore ebb transport from a large onshore flood transport. This observation has also been made by Christie et al. (1999). They performed measurements on a tidal flat in the Humber estuary, but with only one OBS-sensor and one velocity sensor. By assuming a logarithmic velocity profile and depth-constant concentration, they were able to calculate sediment fluxes. They found that maximum sediment fluxes occurred in the shallows (< 0.5 deep, at the beginning and end of immersion), when concentrations and velocities were large. The small residual sediment transport is directed onshore and is determined as the difference between the large values of the ebb and flood fluxes. The same situation probably applies to the Paulina polder, where the largest velocities, turbidities and turbulence also occur in the shallows at the beginning and end of immersion.

4.1.3 Numerical simulations

It was originally planned to carry out simulations with a 1DV model as well. The objective was to simulate a collapse of the concentration profiles. These simulations have not been performed for two reasons:

First, the concentration profiles from the model cannot be validated with the concentration data. Due to an inadequate calibration of the OBS-sensors, the OBS data cannot be used to say something about vertical derivatives (gradients).

The second reason is that the input for the 1DV model requires the average velocity. This parameter could not be extracted from the measured data for two reasons. First, the velocity data show a veering with height during a part of the tide, due to which it is not sensible to fit a velocity profile. Second, in all the 16 Hz data, and some of the 4 Hz data, an erroneous offset existed in one velocity component. This makes is impossible to assess the average velocity (neither magnitude nor direction).

4.2 Recommendations

A further investigation of the veering of the velocity with height as observed in the Paulina measurements is recommended. At present the hypothesis is that the density currents are the result of sediment-fluid interaction. A strategy for further research is to start with sensitivity research with numerical models to find the actual cause for the veering of the velocity with height. It is also recommended to perform a further data analysis. When the cause for the veering has been determined, it is recommended to start a new field measurement campaign to gather the data required to validate this cause in the numerical model simulations.

4.2.1 Numerical simulations

It is recommended to perform a sensitivity analysis by means of numerical 3D-simulations to find the cause for the veering of the velocity vectors with height.

A number of authors have already performed Delft3D simulations of the Paulina salt marsh in the Westerscheldt. All these simulations concerned simplified basins and geometries. Kusters (2003) and Temmerman (2003) performed simulations on a narrow slice of the Paulina marsh: They used a grid with three closed boundaries and one open boundary located on the edge of the main channel. This model does of course not show any rotation of the velocity vectors with the phase of the tide (as observed in figure 7), it is only subject to tidal filling with crosshore velocities. Paarlberg (2003) performed simulations on a more complex Paulina grid. He put the patch of Paulina polder bathymetry used by the previous in a long wide grid. One of the two long sides was closed and represents the main land boundary, the other long side was the main axis of the main channel. The two short sides were located far up and downstream of the salt march patch and were assigned a depth equal to the main channel. The bottom topography gradually increased from these two boundaries up to the level of the salt marsh in the middle of the domain. In this model there is a rotation of the velocity vectors with the ongoing phase of the tide, although the rotation value is not correct. Since the only aim of this study was the simulation of the magnitude of the velocities, this was not an issue. For our purposes however, where we want to model the vertical veering of the velocity, this is not sufficient. Consequently, a whole new model has to be set-up for our objectives. It is possible though to get boundary conditions when nesting our model in the larger ScalWest model.

Besides performing Delft3D simulations to assess the presence of sediment-flow interaction (density currents) at the Paulina polder, it is also recommended to calculate the onshore and offshore fluxes of sediment and compare them to the experimental results of Christie et al. (1999).

4.2.2 Further data analysis

It is recommended to subject the currently available data to a more thorough analysis. The most important recommendations are to correlate the data to (i) to recordings of wave buoys located in the Westerscheldt and (ii) to meteo events:

1. The wave trains which were present in the velocity data are expected to be the caused by ships. Comparison with wave buoy data can support this assumption. It is also recommended to look closer at the magnitude of the orbital velocities near the bed caused by waves, not only the incidental ship wave trains, but also the almost present small wind waves. The bed shear stresses caused by waves are much larger than the bed shear stresses caused by the mean currents. Waves are therefore expected to have a large influence on the mud fluxes.
2. The veering of the velocity with height as observed in the data might be caused by wind. Therefore it would be very useful to compare the measured velocity data to KNMI wind data.

4.2.3 New field measurement campaign

When the cause for the veering of the velocity with height has been determined, it is recommended to start a new field campaign. A few important recommendations should be taken into account:

- The data should be analyzed from the first day on; one should not wait until all data have been collected. If for instance instrument errors are detected, one can take measures right away. This approach will assure that at least the last part of the data series is completely satisfactory.
- One and the same person should be fully responsible for the whole field campaign. This person should be someone not too busy with other obligations. This approach assures that communication takes places on time between and between the right participants. If something might go wrong despite appropriate communication, it is at least clear which person should perform ad hoc actions to save the campaign.
- More than 2 velocity and 2 turbidity sensors should be mounted on the measurement frame. Generally, the velocity on the tidal flat is does not have a vertical logarithmic distribution. For instance, at least three velocity sensors are required to fit a Van Veen velocity profile.
- A thorough calibration of the turbidity sensors should be performed on the site. This calibration should also be repeated quite frequently.

References

Bouma, T.J., M.B. de Vries, L.Custers, E. Low, P.M.J. Herman, I.C. Táncos, A.Hesselink, H. Verbeek, P.Meire, S. van Regenmortel, 2003. preliminary ECSA paper Hydrobiologica. *Identifying the minimal set of measurements needed to characterize mudflat-salt marsh ecosystems in terms of hydrodynamics; a case study on the Paulina polder in the Westerscheldt estuary.*

Christie, M.C., K.R. Dyer and P.Turner, 1999. *Sediment flux and bed level measurements from a macro tidal mudflat.* Estuarine, Coastal and Shelf Science, **49**, p 667-688.

Ham, R. van der, 1999. *Turbulent exchange of fine sediments in tidal flow.* PhD-thesis, Delft University of Technology; also: Delft University of Technology, Faculty of Civil Engineering and Geosciences, Communications on Hydraulic and Geotechnical Engineering, Report No 99-1.

Kusters, L.E.M. march 2003. *Field Data Processing.* Internal Delft Hydraulics Report Z2827.85. Part of M.Sc. thesis.

Kusters, L.E.M. march 2003. *Computer modelling Paulina polder.* Internal Delft Hydraulics Report Z2827.85. M.Sc. thesis.

NRC Handelsblad, 2003. *Zandplaten in Zeeland kalven af.* Article from R. Biersma, 11 november 2003. (in Dutch).

NRC Handelsblad, 2003. *Dam van verzoening' helpt niet tegen afkalving.* Interview by R. Biersma with 'Hoofdingenieur Saeijs' about the Oosterscheldedam. 12 novenber 2003. (in Dutch).

Paarlberg, A.J. 2003. *The significance of biological activity for morphology and sand-mud distribution in the bed.* Internal Delft Hydraulics Report Z2837. M.Sc. thesis.

Smits J., 2003. *Modelling of the sediment-water interaction.* Internal Delft Hydraulics nota.

Temmerman, S. 2003. *Sedimentation and morphodynamics of tidal marshes in the Scheldt estuary: a field and numerical modelling study.* Ph.D thesis KU Leuven.

Vries, Mindert de, april 2003. *R&D Theme 2, Cluster 2.1 Effect-chain Wadden Sea.* Internal Delft Hydraulics nota.

J.C. Winterwerp, (1999). *On the dynamics of high-concentrated mud suspensions.* PhD-thesis, Delft University of Technology; also: Delft University of Technology, Faculty of Civil Engineering and Geosciences, Communications on Hydraulic and Geotechnical Engineering, Report No 99-3.

Winterwerp, J.C. 2002. *The transport of fine sediment in the Wadden Sea. Set-up of the study.* Flyland /ONL Report Z3385.

Winterwerp, J.C., Th. Van Kessel, 2002. *Siltation by sediment-induced density currents.* In: proceedings PECS 2002, Hamburg.

Winterwerp, J.C. 2001. *Stratification effects by cohesive and non-cohesive sediment.* Journal of geophysical research, Vol 106., no. C10, pages 22,559-22,574.

Winterwerp, J.C. *The sedimentation rate of cohesive sediment. Preliminary chapter of book and set-up for paper.*

A Objectives 100 day Pauline polder campaign

This appendix contains some quotations from Bouma et al. about the objectives for setting up a 100 day measurement campaign at de Paulina polder.

"Long-term development of mudflat-salt marsh ecosystems is determined by the interaction between hydrodynamic conditions and sediment (extensively reviewed by Allen 2000; see his Fig. 4). Strong hydrodynamics and lack of sediment will cause mudflat-salt marsh ecosystems to reduce in size due to erosion, whereas high sediment availability combined with low hydrodynamic energy will result in accretion. Hydrodynamic and sediment characteristics are also the main factors determining species habitats on mudflat-salt marsh ecosystems. Sediment characteristics and current velocities have been shown to be important factors in determining the distribution of benthic organisms in estuaries (Ysebaert et al. 2002), whereas inundation period and wave energy are important factors in explaining the distribution of plant species along the elevational gradient (de Leeuw et al. 1992, Houwing 2000).(...)

In general, few detailed experimental observations exist on the hydrodynamic conditions of mudflat-salt marsh ecosystems, especially in European marshes (review Allen 2002). Studies that relate important ecological principles to hydrodynamic factors often use semi quantitative methods to measure hydrodynamics such as the dissolution block technique (e.g. Bruno 2000). Due to technical limitations related to translating these types of measurements into rates (Porter et al 2000), use of such semi quantitative methods complicates comparing data of different studies. Alternatively, ecological studies may use data from hydrodynamic models, which often have relative large grid sizes (generally 100 m grid, however sometimes as fine as 30 m grid; see e.g.. Ysebaert et al. 2002, Herman et al. 2001). A major complication in using such models is that they are developed for subtidal areas, which are much deeper than mudflats and salt marshes. This causes especially problems with respect to the differences in bottom roughness when simulating shallow areas. Summarising we conclude that

A. identifying the minimal set of measurements needed to characterise mudflat-salt marsh ecosystems in terms of hydrodynamics would be an important contribution to ecological studies of these ecosystems, especially because hydrodynamic conditions may strongly differ locally depending on wind exposure and tidal amplitude and
B. having a long-term data set would be valuable for calibrating existing hydrodynamic models for shallow areas such as mudflats and salt marshes.

Hence, the objective of our present study is to address these two points by collecting a long-term high-resolution hydrodynamic data set that allows hydrodynamic description of a mudflat-salt marsh ecosystem in an estuary, including the creeks that run into the salt marsh. This data set will be used for

1. identifying general relationships that can be used for habitat characterisations at other locations
2. calibration of existing hydrodynamic models for shallow areas such as mudflats and salt marshes,
3. defining realistic conditions in our flume studies on ecosystem engineering by plants and animals,

4. modelling of hydrodynamic sediment transport over the mudflat-salt marsh ecosystems and
5. modelling of long-term development of mudflat-salt marsh ecosystems. In this paper we focus on the first point.

As field site we choose Paulinapolder in the Westerschelde estuary (SW Netherlands), which is characterised by a large mudflat and a salt marsh with an extended and viable zone of pioneer vegetation mainly consisting of Spartina anglica. To our knowledge, no long-term high-resolution hydrodynamic data set exists for any of the Westernschelde mudflat-salt marsh ecosystems."

B Technical details DON frame

The high and low- frequency data sets were both collected in the same way at the DON (Directie Oost-Nederland) frame. The only difference was the sampling rate and the burst length.

B.1 DON frame Location

In this section the co-ordinates of the frame are given in table B.1 Figures B-1 to B-4 show the location and environment of the frame.

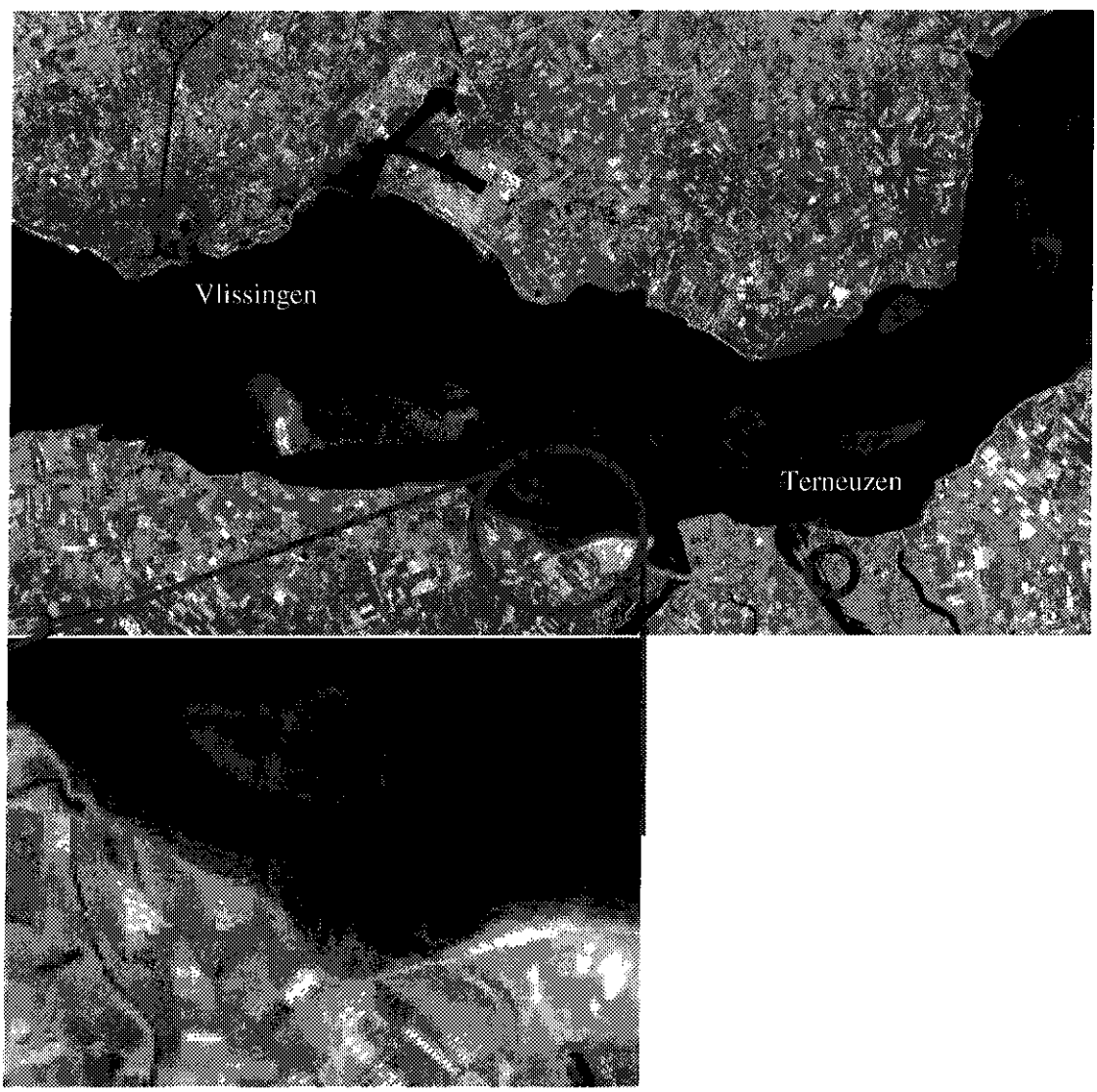

Figure B-1. Satellite image of Westerscheldt with Paulina polder. *Source (http://satfoto.dhp.nl/).* Note that the site is protected from waves by a number of sand plates.

	Value	Description
x	38862.17	[m] Parisian coordinates
y	374881.89	[m] Parisian coordinates
z	0.5638	[m] NAP

Table B-1

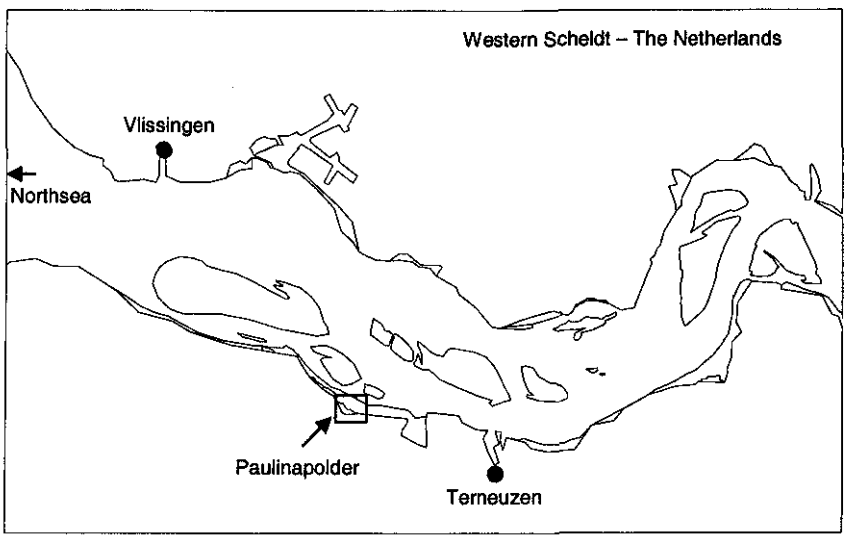

Figure B-2. Map of Westerscheldt with Paulina polder.

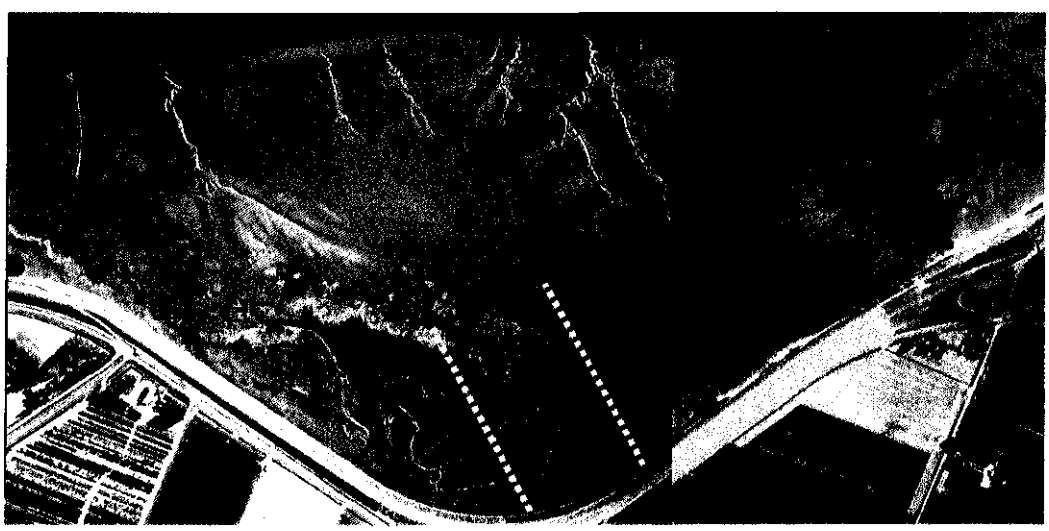

Figure B-3. Aerial picture Paulina polder (*note: vertical of picture not aligned with North-South axis*). Dashed lines approximately indicate bottom profile in next figure.

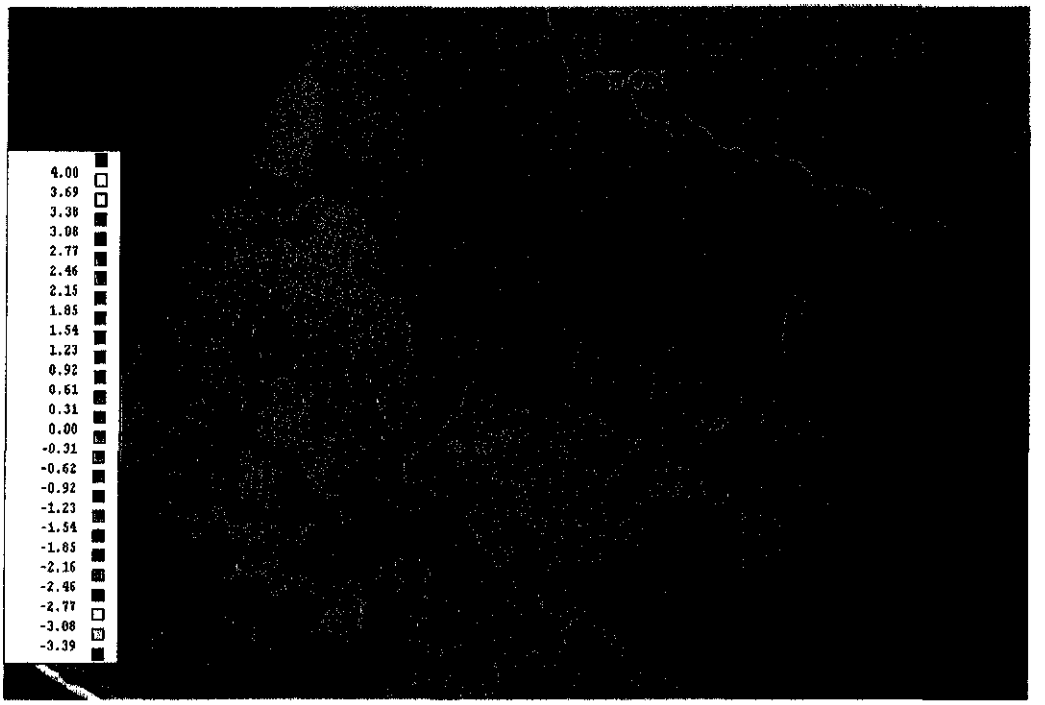

Figure B-4. Bottom Topography Paulina polder and location measurement devices.

B.2 Instruments

The DON frame was equipped with velocity, turbidity and water level sensors (see figure B-6 and table B-2).

Parameter	Datastream name	Sensor Name	Polarity	Sampling rate	Height
Velocity	EMF1		apems	4Hz	0.15 [m] above bottom
	EMF2		pems	4Hz	0.07 [m] above bottom
Turbidity	OBS1	382	-	4Hz	0.25 [m] above bottom
	OBS2	383	-	4Hz	0.15 [m] above bottom
Water level	druksens		-	1 minute	0.13 [m] above bottom

Table B-2. OBS = Optical back Scatter, EMF = Electro magnetic Flow meter.

The instruments measure a data stream and write it to disk. This written data stream may contain several anomalies. These can either originate from instruments characteristics, or from underlying physical behaviour. Both an experienced physicist and an experienced instrument builder are needed for interpreting the data and attributing the anomalies to either the physics (so it will have to be explained) or to the instruments (so the data can be thrown away). Several such anomalies have been encountered: noisy signals during ebbing and flooding, concentration peaks due to waves, an offset in one of the velocity components.

Noisy signals during ebbing and flooding
All sensors measure both in air, when they are dry, and in water, when they are submerged. In the velocity and OBS measurements the transition from air to water (both during flooding and ebbing) cannot easily be inferred from the signals itself in an automated process, since there is no criterion available which could detect the transition from air to water. Moreover, the transition is not smooth, but very 'grassy'. First, during the actual submerging, which

takes several minutes, the sensor is alternatingly dry and wet due to small waves. The recorded signal is therefore very noisy during this period. Secondly, when the sensor becomes dry for a short period (between two small waves), drops of water still hang from the sensor, thus blurring the signal. Third, even correct signals are very noisy during drying and flooding since lots of turbulence is generated in the peeling tidal wave, entraining lots of sediment. Distinguishing real noisy signals from artificial noisy signals can be overcome by using the pressure data stream as a mask for the velocities and the turbidity. However, due to two reasons the pressure sensor data cannot directly and unambiguously be used as a mask for the velocity and turbidity data. First, the pressure data has to be corrected for atmospheric pressure fluctuations. A 1 mbar variation (on the average atmospheric pressure of order 1000 mbar) in the air pressure leads to a 1 cm difference in water level. Second, the different sensors are placed at a different levels on the frame, and accordingly drown and dry at different moment. Consequently there is a phase difference between the water level mask and the OBS/EMF data stream it is meant to mask.

Figure B-5. DON frame

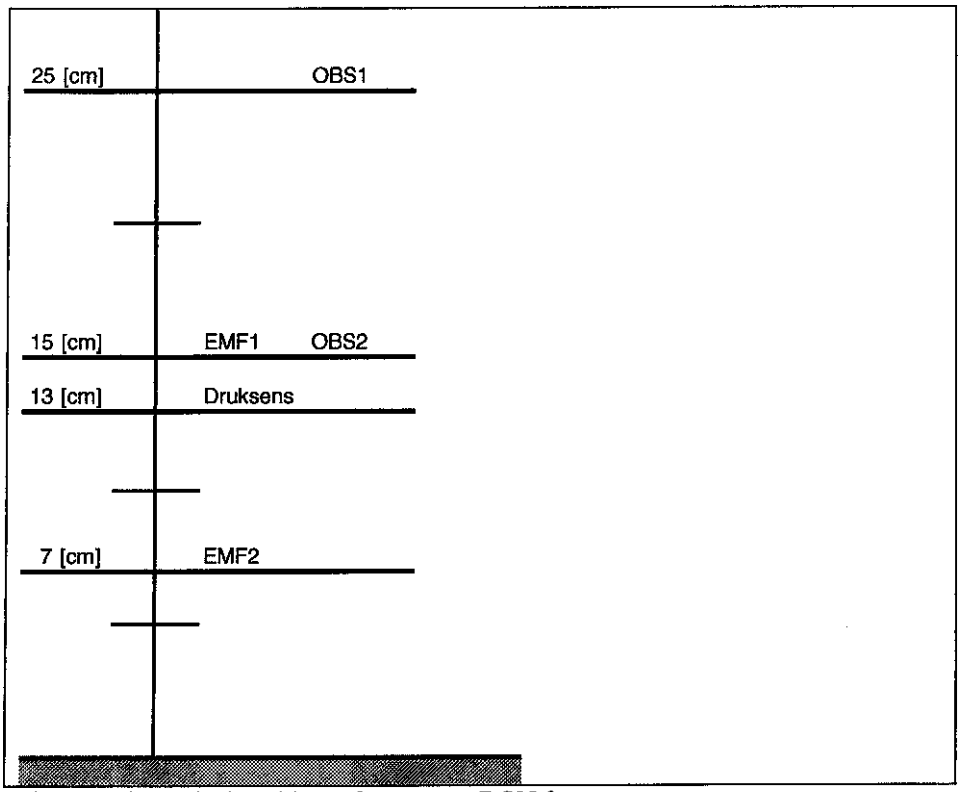

Figure B-6. Vertical position of sensors at DON frame.

B.3 Data storage

All data were directly stored in files at the site of measurement. The data were written in specially designed digital form in order to minimize the size of the data storage. This was quite useful since the size of the data was one of the limiting factors for long-term measurements (besides battery supply). These digital files had to be converted to human readable ASCII files with a special program, which knew the exact digital coding.

The measurement of one tide is covered with a 6 hour semi-continuous measurement span. The 6 hour tidal recording periods are split up in units of 8 logs, which are written to separate files, each file containing 45 minutes of data. The 6 hour time span is sufficient to record the entire period that the marsh is flooded. This approach saves valuable disk space (measuring in air is not very useful). Moreover, between the recordings of two consecutive tides the frame is even put in stand-by mode to save energy (batteries) as well. A timer is present in the DON frame to ensure that after such a stand-by period, the frame is switched on and started up again on time for the next tide (which is after 6:15 or 6:30 minutes).

The above method undoubtedly solves an enormous amount of data storage problems and energy supply lacks. However, a part of the data set is collected in such a way that either the start of flood, or the end of ebb are not measured. These are the most interesting part of the tide, since most of the sediment is transported in the highly turbulent ebb or flood 'bores'. This happens most often just after the frame has been accessed by personnel for maintenance, new batteries or data retrieval. Another reason which contributes to this is that the frame cycle and the tidal cycle don't have exactly the same frequency. This phase difference between the tide and the DON frame changes in time, so the tide can shift out of

the measured time window. In next expeditions, more attention should be paid to a proper timing of the shut-down of the frame, as it causes an unfortunate loss of data.

Each of the 45 minutes DON files contains three measurement bursts covering 15 minutes each. (More precise: the time between the start of two consecutive bursts equals 15 minutes.) Each of these 15 minute-bursts contains of 2048 lines of data (containing the OBS, EMF and pressure data). These data are sampled at 4 Hz, which means that 2048 lines represent 512 [sec] of data (2048 / 4 [Hz]). (equivalent to 8 minutes and 32 seconds). Since the next burst does not start until 15 minutes after the start of the previous, this implies that between two subsequent burst 6 m 28 s (15 m minus 8 m 32 s) are not covered with data. This is the second approach adopted to save valuable disk space (besides the shut-down between two tides).

The data reduction method leads to a decrease of 43 % of the file sizes. However, it also has two unforeseen, but unfortunate consequences. First, the shattering of the time axis into the small 8 m 53 s domains severely limits the freedom possibility of extracting various turbulence properties from the data. Moreover, it also removes parts of very interesting short term incidents from the data series. The effect of a wave train entraining some sediment and the subsequent settling of it, which is a 30 minute event, cannot be traced properly in the chopped time frame. The measurement campaign was not set-up to yield turbulence and in-detail short term recordings, and is as such not to be blamed for these unfortunate choices. However, it is always useful to be aware of positive side advantages of any measurement effort.

Column Position	Code ID100	Code ID200	Code ID300/301
1	ID 100	ID 200	ID 300
2	Raw EMF_1X	Day julday	Day julday
3	Raw EMF_1Y	Hour/Minute hhmm	Hour/Minute hhmm
4	Raw EMF_2X	Average Kompas	Average EMF_1X
5	Raw EMF_2Y	Average Tilt_X	Standard Deviation EMF_1X
6	Raw OBS_1	Average Tilt_Y	Average EMF_1Y
7	Raw OBS_2	Average Batt__24V	Standard Deviation EMF_1Y
8	Raw Druksens	Average Batt_CR10	Average EMF_2X
9	-	Average Temp_CR10	Standard Deviation EMF_2X
10	-	-	Average EMF_2Y
11	-	-	Standard Deviation EMF_2Y
12	-	-	Average OBS_1
13	-	-	Standard Deviation OBS_1
14	-	-	Average OBS_2
15	-	-	Standard Deviation OBS_2
16	-	-	Average Druksens
17	-	-	Standard Deviation Druksens

Table B-3. Data line coding in DON files.

Each of the three 15 minute data blocks in the ASCII files start with a line labelled with (starting with) code 200, while the three blocks of 2048 actual data lines are labeled start with code 100 (see table B-3). This '200'-line contains meta-data about the instruments (see table B-3), the most important of which is the start time of the data block. However, sometimes the first block does not start with such a line. This is not a problem as such, since the start time of this block can be inferred form the start time of the next block. However,

when implementing automatic processing of the data, the random absence of this line requires troublesome solutions. It is therefore recommended to make the file structure as predictable and standard as possible.

The aim of the campaign was to get the burst means. The measuring device was programmed to calculate these means, as well as the standard deviations of each burst directly. The means were calculated per 8 min and 53 sec burst. These data labelled with 300 (see table B-3) and were written to a separate file. In this file the mean was calculated irrespective of whether the underlying high frequency data were correct. Therefore at least the first and last mean data point of every tide must be skipped. To remedy this shortcoming a Matlab post processing tool has been written which calculates the average and plots it together with the underlying data, thereby increasing the understanding of the data.

B.4 Velocity calibration

The calibration curves for the velocities are:

$$Velocity\_x1[m/s] = (5/2949) * (EMF1\_X - 6) \quad \text{(B-1)}$$

$$Velocity\_x2[m/s] = (5/3017) * (EMF2\_X - 5) \quad \text{(B-2)}$$

$$Velocity\_y1[m/s] = (5/2398) * EMF1\_Y \quad \text{(B-3)}$$

$$Velocity\_y2[m/s] = (5/2378) * (EMF2\_Y + 31) \quad \text{(B-4)}$$

where EMF(1/2)_(X/Y) are the measured signals in mV. The EMF velocity sensors give a signal in both the x and y direction. EMF sensors have a polarity: they can either be P-EMS or aP-EMS (see figure B-7), which means a flipping of the y direction. Consequently, for the lowest sensor, EMF2, the x data stream has to be multiplied with –1. For the DON frame, the x axis in the field was aligned by pointing it at the nuclear power station Borssele, while the y velocity was rotated by 90 degrees to the right with respect to the x direction in a plan view (i.e. +90 degrees in a Cartesian grid). The coordinates of the Borssele nuclear power and the DON framed plant are listed in table B-4.

Co-ordinate	Value		Lat-lon
X	37666.324	[m] Parisian coordinates Borssele	51 06 00 N
Y	383949.297	[m] Parisian coordinates Borssele	03 42 00 E
X	38862.17	[m] Parisian coordinates DON frame	
Y	374881.89	[m] Parisian coordinates DON frame	
Z	0.5638	[m] NAP DON frame	

Table B-4. Co-ordinates Borssele nuclear power plant and DON-frame.

Applying the coordinates in table B-4 gives an angle of 7.5 degrees between the x velocity of the frame and the true North. Moerover, the shore line of the salt marsh also makes an angle with the true north (figures B-1 and B-4). This angle is about 30 degrees. Transforming to these directions should therefore be done by rotation over 37 deg. The following geometrical relation, which can be found in many a math text book, has to be used for rotation of the data:

$$\begin{pmatrix} U \\ V \end{pmatrix} = \begin{bmatrix} \cos(\alpha) & -\sin(\alpha) \\ \sin(\alpha) & +\cos(\alpha) \end{bmatrix} \begin{pmatrix} u' \\ v' \end{pmatrix} \tag{B-5}$$

where u' and v' are the measured velocity components, U and V are the desired velocity components and α is the angle between the measured x velocity component and the desired Cartesian grid one wants to map the velocities onto. One example of a rotated time series of the velocities is displayed in fig B-8 for three different coordinate systems.

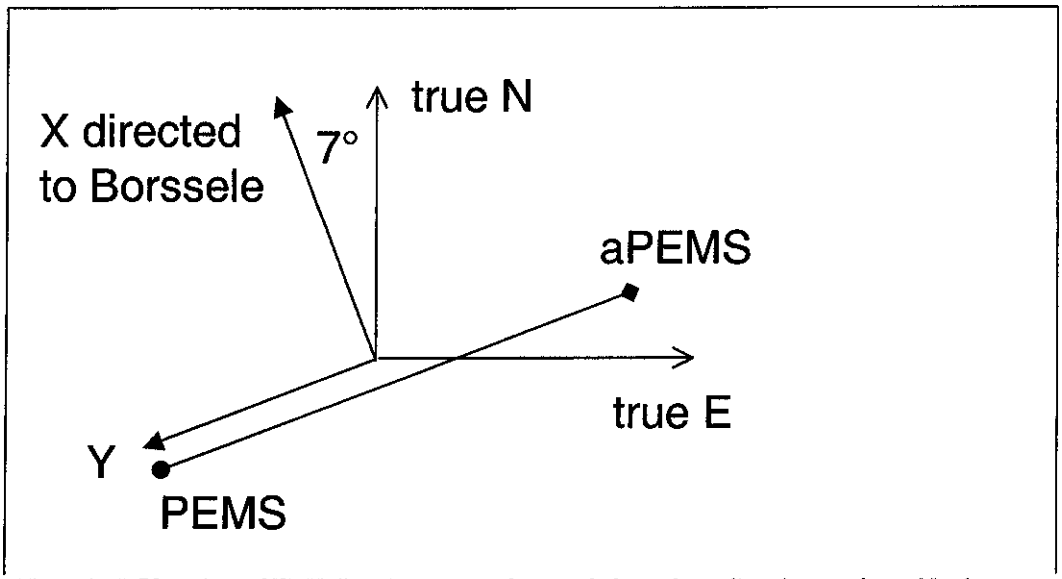

Figure B-7. Plan view of EMF directions, cross shore and along shore directions and true North.

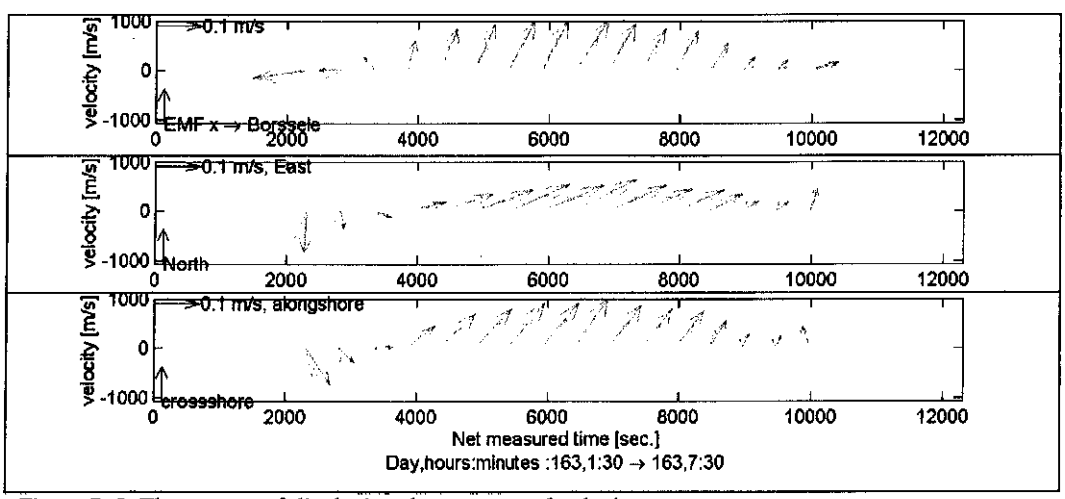

Figure B-8. Three types of displaying the same set of velocity vectors:
Original data with x directed to Borssele, y rotated with -90 degrees.
y aligned with true North, x with East
x directed alongshore local upstream direction, y directed cross shore

B.5 Turbidity calibration

The turbidity values at 25 cm were higher than the values near the bottom (15 cm). Therefore it was decided to invest in a thorough recalibration of the OBS sensors with an original mud bed sample collected at the very time of the measurements. This recalibration was improved with respect to the original one by:

Using multiple concentrations (4 concentrations: ranging from clear water to almost 2 g/l)

Allowing an offset on the (OBS [mV] – c [mg/l]) calibration curve.

Using the average of a recorded 5 minute OBS time series registration rather than estimating the OBS signal from the fluctuating display as is normally done.

The results of the calibration (table B-5) are shown in figure B-8 to B-11 together with the least square fit.

No.	Empty weight	Total weight	Net weight	Sample	Volume	Concentration	OBS1	OBS2
	[gr]	[gr]	[gr]	[nr]	[ml]	[mg/l]	[mV]	[mV]
demi	water						27	21
137	0,1122	0,1185	0,0063	b3501-012	240	26,25	39	32
138	0,1134	0,1336	0,0202	b3501-028	257	78,60	68	57
139	0,1011	0,5109	0,4098	b3501-068	250	1639,20	644	564

Table B-5

The calibration on the data in table B-4 gives the following results, with coefficients given in table B-6.

$$OBS_1 = a_1 + b_1[mV] \quad \text{(B-6)}$$

$$OBS_2 = a_2 + b_2[mV] \quad \text{(B-7)}$$

least square fit	a1	b1	a2	b2
only 3 lowest data points	-85.5	2.70	-75.5	3.06
all 4 data points	-49.2	1.87	-47.4	2.27
least square fit	a1	b1	a2	b2

Table B-6

However, even after this thorough recalibration is applied to the data, the near bed concentrations are still lower than the ones higher in the water column. This difference is very sensitive to the small offset in the calibration curve however.

The option that errors were made in the registration, for instance swapping of cables, calibration curves or data streams, has also been investigated. The small phase difference present in the flooding time of the two sensors reduced the number of error paths to be investigated. The remaining options gave even worse results than the no-error scenario. Therefore it was concluded that the measurements have been carried out correctly.

It can be concluded that for OBS -collected turbidity data, a thorough calibration at the very site itself is mandatory; calibration afterwards does not work, even if the same sediment sample is used.

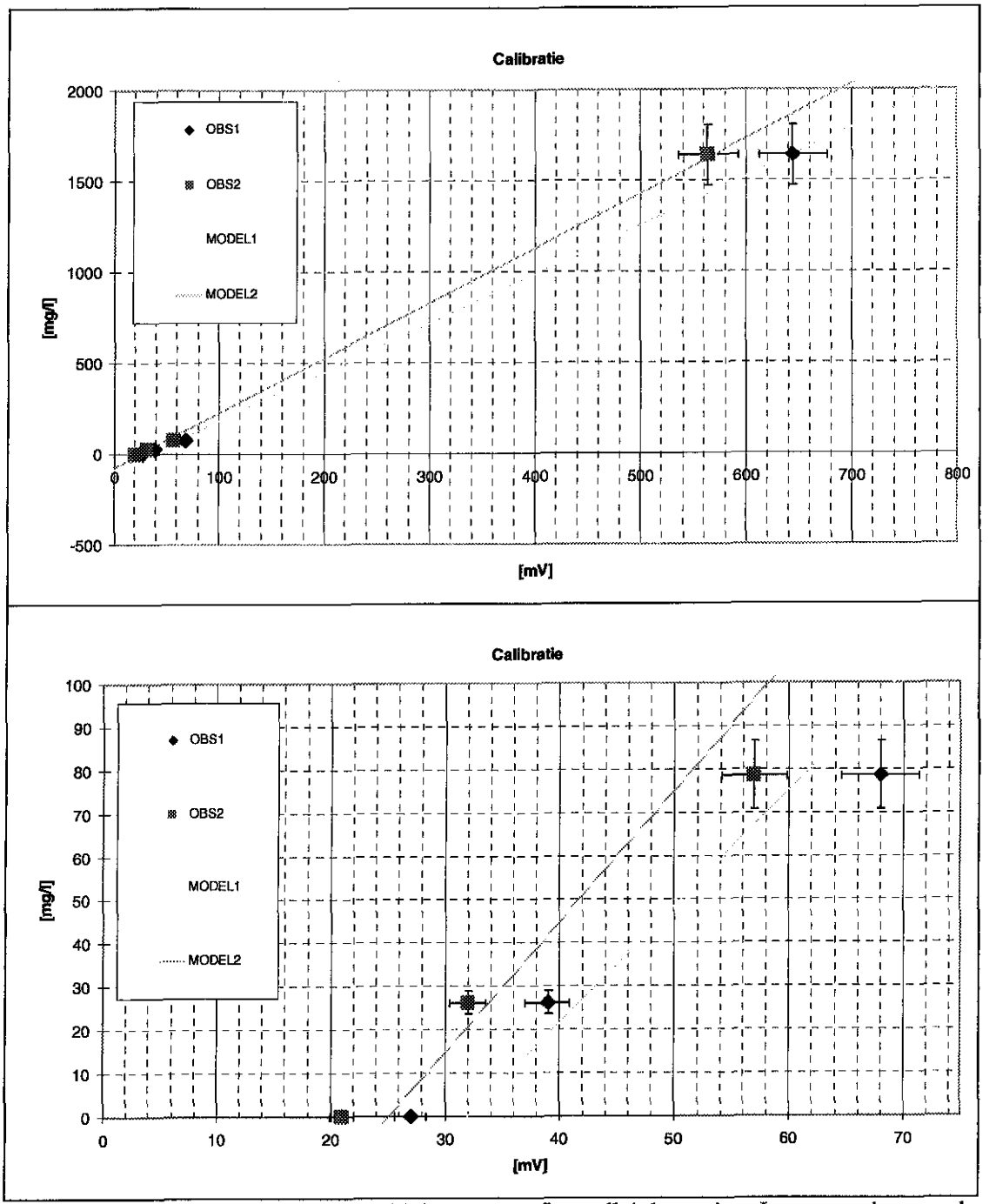

Figure B-9. Turbidity calibration with least square fit on all 4 data points. Lower panel: zoomed in on 3 low-concentration data points.

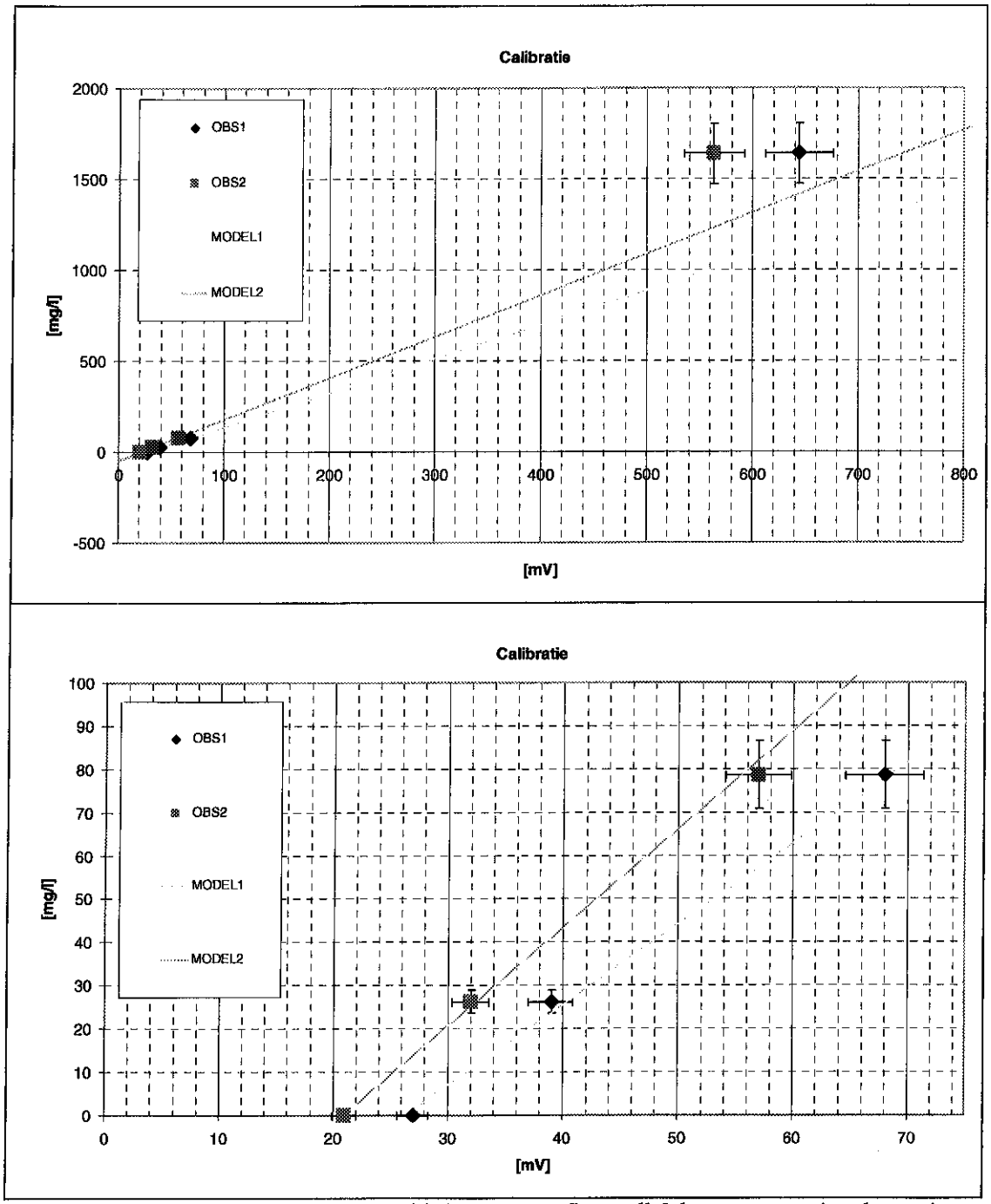

Figure B-10. Turbidity calibration with least square fit on all 3 low-concentration data points. Lower panel: zoomed in on 3 low-concentration data points.

B.6 Water level calibration

The water level sensor is a pressure gauge. It gives the total pressure: i.e. the atmospheric pressure plus the water pressure. The atmospheric pressure is subject to high and low pressure systems. These can vary in the most extreme cases from say 990 mbar to 2030 mbar. The data should be corrected for this abbreviation. Time series of air pressure from KNMI can be used for this. This correction has not been applied in this study however. The calibration curve for the water level reads:

$$Pressure[mBar] = 1000 + (0.24203 * druksens) \quad \text{(B-8)}$$

B.7 Data processing

In order to facilitate the processing of the huge amount of 4Hz data (over 1300 ASCII files !) a series of matlab script has been written to enable automatic processing. The main difficulty was to deal with all the missing and corrupt data.

1. A small data base off all potentially available data files has been made. This was written to an ASCII table. For this, each data file was first checked for presence and size and assigned a flag. Then all remaining files were checked for error and also flagged of if necessary. This result was written to a matlab readable file.
2. The meta information (time) of all correct files was read and put into the data base.
3. All data were read with the use of the data base, transformed to the correct SI units , masked, and written to a digital matlab file (to reduce disk storage and increase access time).
4. The digital data was read in matlab to extract, among other, average values.
5. A batch visualizing script was written in matlab, which read all the digital data, and wrote it to an image file.

Based on the above experience a few recommendations are given:

Existing or simple formats for writing data to ascii files should be used:

- E.g. rectangular ascii files (full rows and columns with dummy values)
- E.g. *.map files

The data from the DON frame were written to comma-separated files, which were difficult to read for a person (no visible columns).

- A specific dummy value for missing values should be required.
- Use a fixed column width for ASCII files to enable fast human inspection of these files. In the DON files, not all the rows contained the same number of rows. This made it less easy to read them into matlab.

Meta data should not be mixed with the actual data itself, but should be contained (i) in a header which is commented out and (ii) in a meta data file.

All necessary information (meta data) should be put in the header of the data files: times, calibration curves, etc.

Make sure that each filename is uniquely related to one measuring burst by putting the time in the filename. The question whether there were data missing for a specific period becomes then very easy (i.e. to inquire the existence of a certain file). For the DON data, specific periods were included in separate directories. These directories all contained the same file names.

B.8 Data analysis

- From the 16 Hz velocity data power spectra have been made. The Matlab function *pwelch* has been used for performing this operation.
- The time window chosen for making power spectra is chosen 660 sec (11 minutes). This time is considered long enough to yield enough information in the low-frequency range

and short enough to be able to assume the underlying processes stationary. A further analysis of the assumption that the signal is stationary has not been performed though.

- The data have been measured at 16 Hz. This means that the highest frequency in the power spectrum will be 8 Hz (Nyquist frequency).
- In *pwelch* the 11 minute time window is divided into a integer number of 50% overlapping (Hamming) subwindows. For each of these subwindows a separate power spectrum is determined. This is generally done to remove noise from the power spectrum. All power spectra in the 11 minute time window are then averaged to yield to spectrum for the entire 11 minute time window. This means that the lowest frequency in the power spectrum is not 1/660 Hz , but has a larger value corresponding to the length of the subwindows. I chose subwindows with a length of 25% of the total window: 165 sec.. This gives a number of 8 subwindows. The lowest frequency is 4/660 Hz = 0.0061 Hz in this case
- The Power spectrum can be calculated very efficiently with an FFT algorithm when the subwindow contains a number of elements which equals exactly a power of 2 (e.g. 2,4,8,16,32 etc.). The length of the subwindow is generally not equal to a power of two. The signal is therefore padded with zeros until is has a length equal to the first power of two larger than the length of the signal. Due to approach, the lowest frequency in the power spectrum is 0.0039 (1/256) Hz (256 s = 4.2 minutes), rather than 0.0061 (4/660 Hz). This first frequency should not be trusted though. The first reliably power density is to be found at twice this frequency: 0.0078 Hz.